Defect Dynamics in an Oscillatory Reaction-Diffusion Equation

Jonathan A. Sherratt

Department of Mathematics
Heriot-Watt University

Dynamics of Patterns Day, Amsterdam, November 26, 2008

This talk can be downloaded from my web site
`www.ma.hw.ac.uk/~jas`

This work is in collaboration with:

Matthew Smith

(Microsoft Research Ltd., Cambridge)

Jens Rademacher

(CWI, Amsterdam)

Outline

Outline

Habitat Boundaries in Ecology

- Ecological habitats are often surrounded by unfavourable environments
- Examples: a wood surrounded by open terrain
  moorland surrounded by farmland
  marsh surrounded by dry ground
- An appropriate boundary condition is "population density=0"

Example: Red Grouse on Kerloch Moor

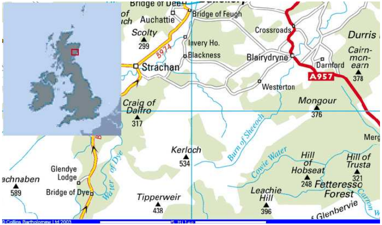

- Red grouse is a cyclic population (period 4-6 years)
- The study site is moorland, with farmland at its Northern edge
- Farmland is very hostile for red grouse

Second Example: Field Voles in Kielder Forest

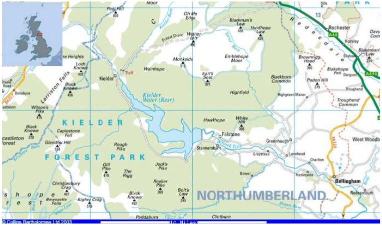

Field voles in Kielder Forest are also cyclic (period 4 years)

Boundary Condition at the Reservoir Edge

- Voles are an important prey species for owls and kestrels
- The open expanse of Kielder Water will greatly facilitate hunting at its edge

Short eared owl

Common kestrel

Boundary Condition at the Reservoir Edge

- Voles are an important prey species for owls and kestrels
- The open expanse of Kielder Water will greatly facilitate hunting at its edge
- Therefore we expect very high vole loss at the reservoir edge, implying that a suitable boundary condition is "vole density=0"

Periodic Travelling Waves in Red Grouse & Field Voles

Spatiotemporal data shows that both red grouse cycles on Kerloch Moor and field vole cycles in Kielder Forest are spatially organised into a periodic travelling wave (wavetrain)

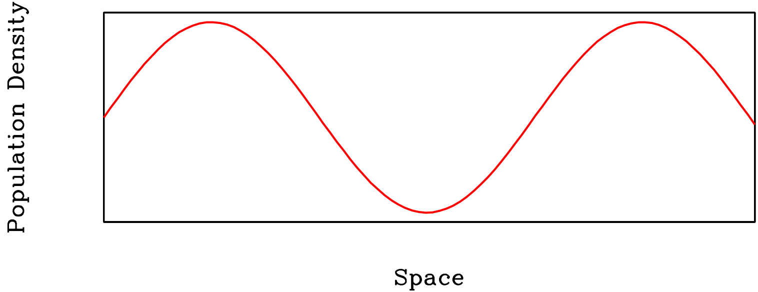

Periodic Travelling Waves in Red Grouse & Field Voles

Spatiotemporal data shows that both red grouse cycles on Kerloch Moor and field vole cycles in Kielder Forest are spatially organised into a periodic travelling wave (wavetrain)

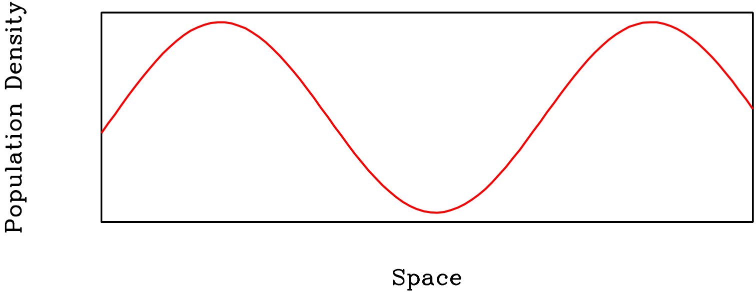

Periodic Travelling Waves in Red Grouse & Field Voles

Spatiotemporal data shows that both red grouse cycles on Kerloch Moor and field vole cycles in Kielder Forest are spatially organised into a periodic travelling wave (wavetrain)

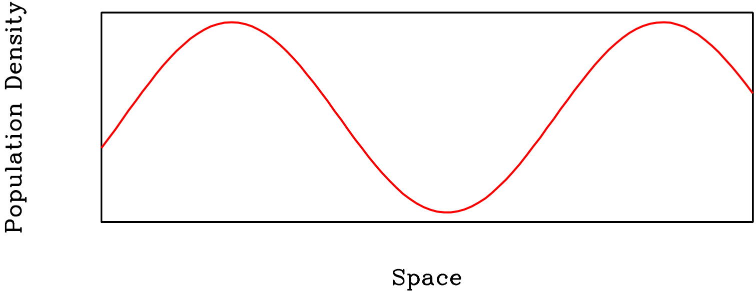

Periodic Travelling Waves in Red Grouse & Field Voles

Spatiotemporal data shows that both red grouse cycles on Kerloch Moor and field vole cycles in Kielder Forest are spatially organised into a periodic travelling wave (wavetrain)

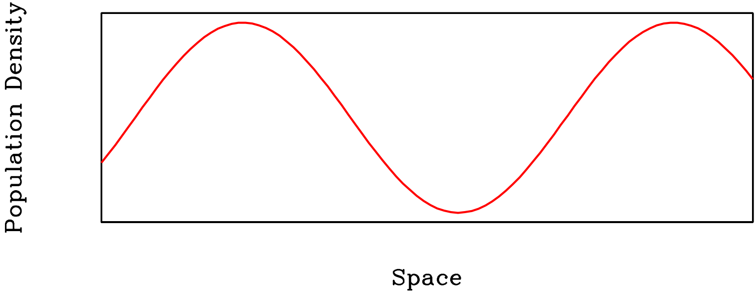

Periodic Travelling Waves in Red Grouse & Field Voles

Spatiotemporal data shows that both red grouse cycles on Kerloch Moor and field vole cycles in Kielder Forest are spatially organised into a periodic travelling wave (wavetrain)

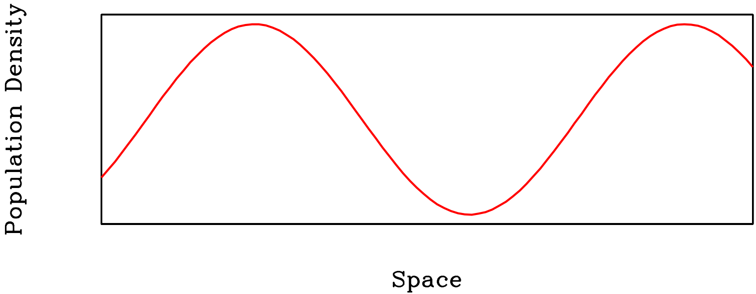

Periodic Travelling Waves in Red Grouse & Field Voles

Spatiotemporal data shows that both red grouse cycles on Kerloch Moor and field vole cycles in Kielder Forest are spatially organised into a periodic travelling wave (wavetrain)

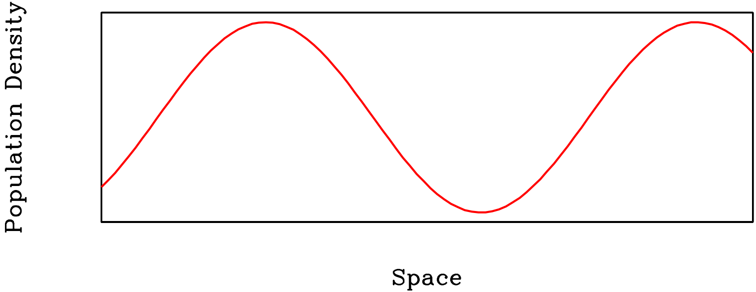

Periodic Travelling Waves in Red Grouse & Field Voles

Spatiotemporal data shows that both red grouse cycles on Kerloch Moor and field vole cycles in Kielder Forest are spatially organised into a periodic travelling wave (wavetrain)

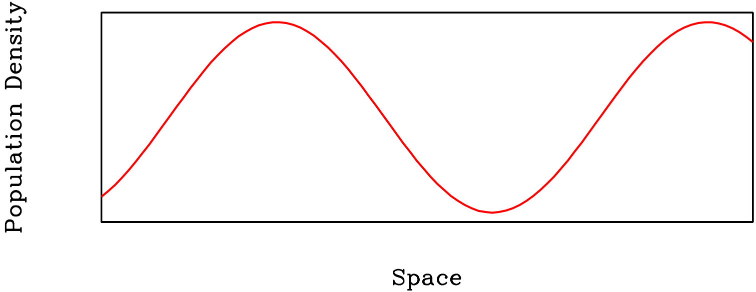

Periodic Travelling Waves in Red Grouse & Field Voles

Spatiotemporal data shows that both red grouse cycles on Kerloch Moor and field vole cycles in Kielder Forest are spatially organised into a periodic travelling wave (wavetrain)

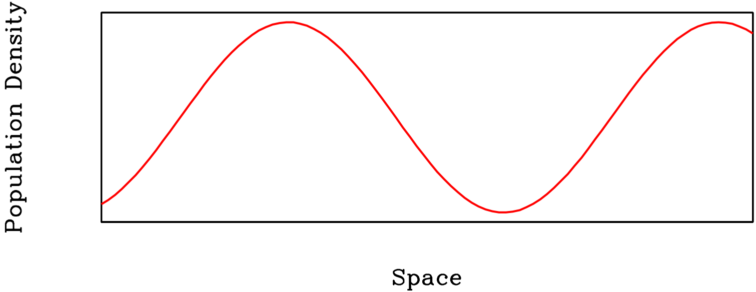

Periodic Travelling Waves in Red Grouse & Field Voles

Spatiotemporal data shows that both red grouse cycles on Kerloch Moor and field vole cycles in Kielder Forest are spatially organised into a periodic travelling wave (wavetrain)

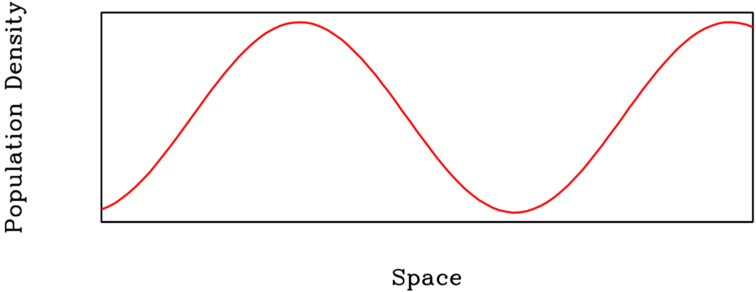

Periodic Travelling Waves in Red Grouse & Field Voles

Spatiotemporal data shows that both red grouse cycles on Kerloch Moor and field vole cycles in Kielder Forest are spatially organised into a periodic travelling wave (wavetrain)

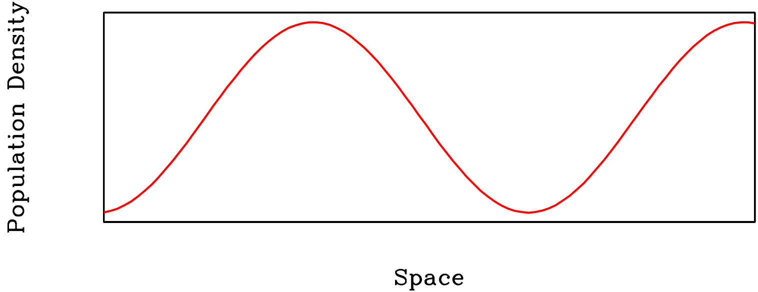

Periodic Travelling Waves in Red Grouse & Field Voles

Spatiotemporal data shows that both red grouse cycles on Kerloch Moor and field vole cycles in Kielder Forest are spatially organised into a periodic travelling wave (wavetrain)

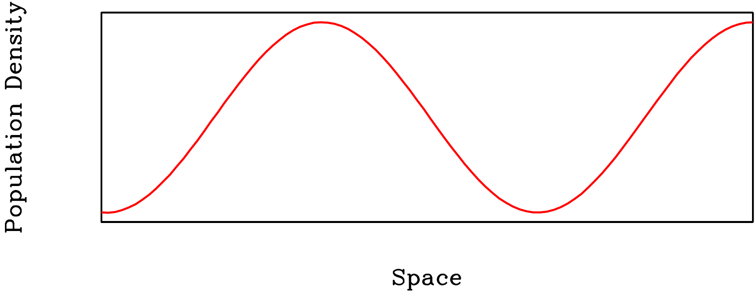

Periodic Travelling Waves in Red Grouse & Field Voles

Spatiotemporal data shows that both red grouse cycles on Kerloch Moor and field vole cycles in Kielder Forest are spatially organised into a periodic travelling wave (wavetrain)

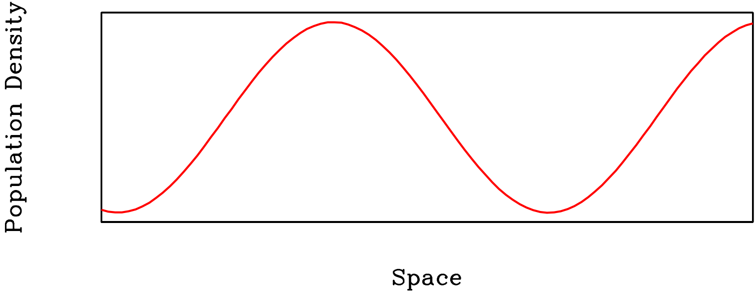

Periodic Travelling Waves in Red Grouse & Field Voles

Spatiotemporal data shows that both red grouse cycles on Kerloch Moor and field vole cycles in Kielder Forest are spatially organised into a periodic travelling wave (wavetrain)

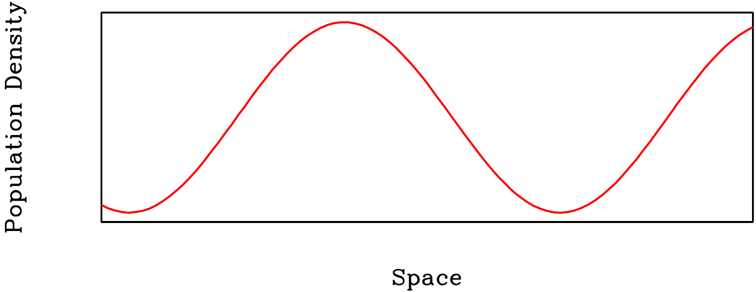

Periodic Travelling Waves in Red Grouse & Field Voles

Spatiotemporal data shows that both red grouse cycles on Kerloch Moor and field vole cycles in Kielder Forest are spatially organised into a periodic travelling wave (wavetrain)

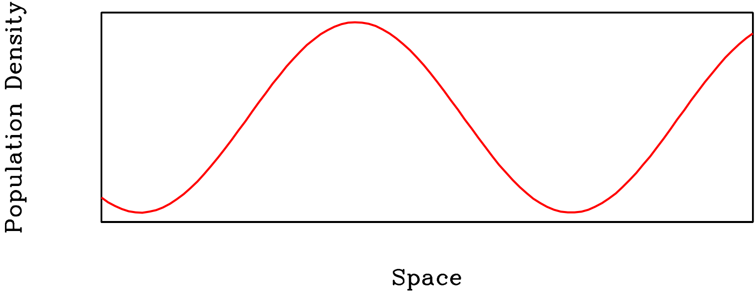

Periodic Travelling Waves in Red Grouse & Field Voles

Spatiotemporal data shows that both red grouse cycles on Kerloch Moor and field vole cycles in Kielder Forest are spatially organised into a periodic travelling wave (wavetrain)

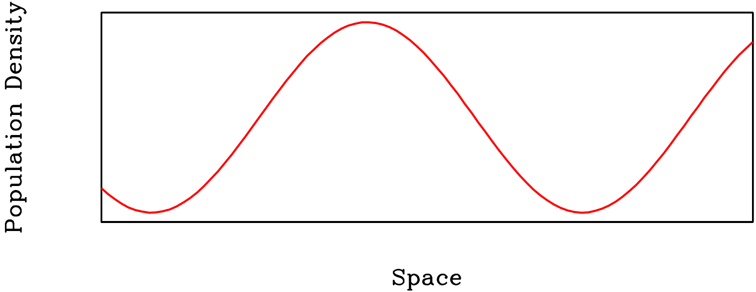

Periodic Travelling Waves in Red Grouse & Field Voles

Spatiotemporal data shows that both red grouse cycles on Kerloch Moor and field vole cycles in Kielder Forest are spatially organised into a periodic travelling wave (wavetrain)

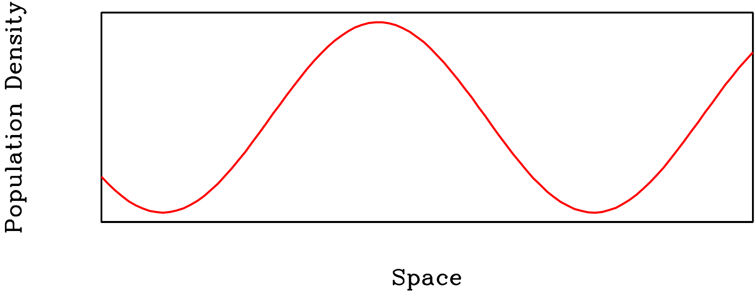

Periodic Travelling Waves in Red Grouse & Field Voles

Spatiotemporal data shows that both red grouse cycles on Kerloch Moor and field vole cycles in Kielder Forest are spatially organised into a periodic travelling wave (wavetrain)

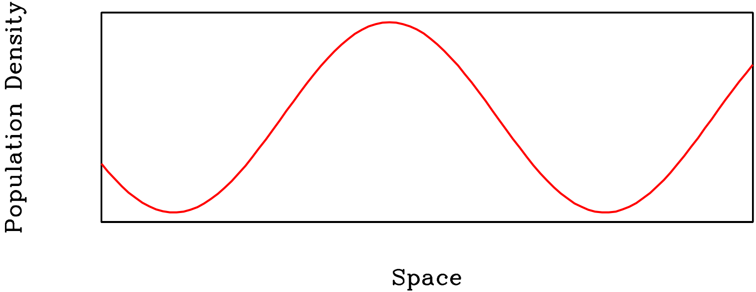

Periodic Travelling Waves in Red Grouse & Field Voles

Spatiotemporal data shows that both red grouse cycles on Kerloch Moor and field vole cycles in Kielder Forest are spatially organised into a periodic travelling wave (wavetrain)

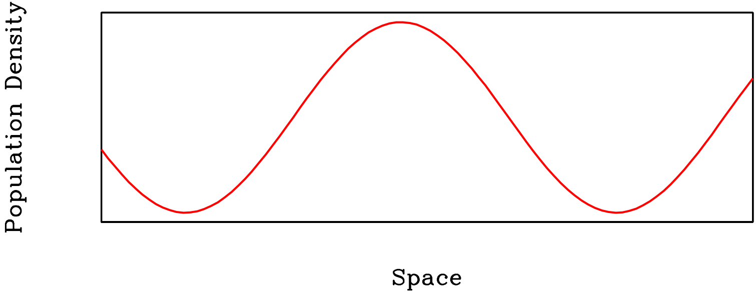

Periodic Travelling Waves in Red Grouse & Field Voles

Spatiotemporal data shows that both red grouse cycles on Kerloch Moor and field vole cycles in Kielder Forest are spatially organised into a periodic travelling wave (wavetrain)

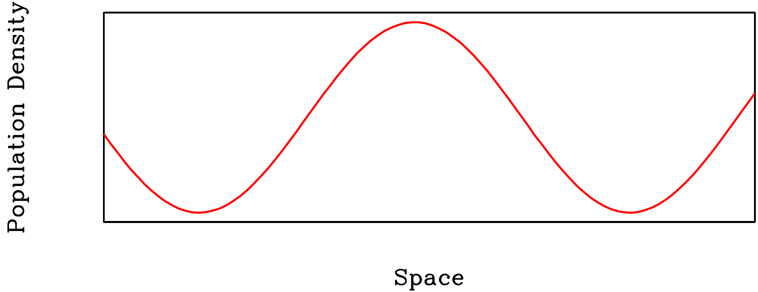

Periodic Travelling Waves in Red Grouse & Field Voles

Spatiotemporal data shows that both red grouse cycles on Kerloch Moor and field vole cycles in Kielder Forest are spatially organised into a periodic travelling wave (wavetrain)

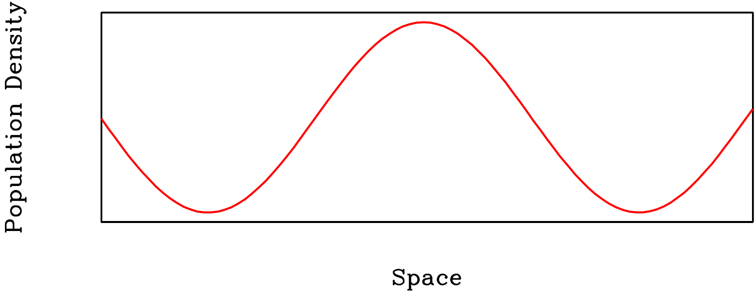

Periodic Travelling Waves in Red Grouse & Field Voles

Spatiotemporal data shows that both red grouse cycles on Kerloch Moor and field vole cycles in Kielder Forest are spatially organised into a periodic travelling wave (wavetrain)

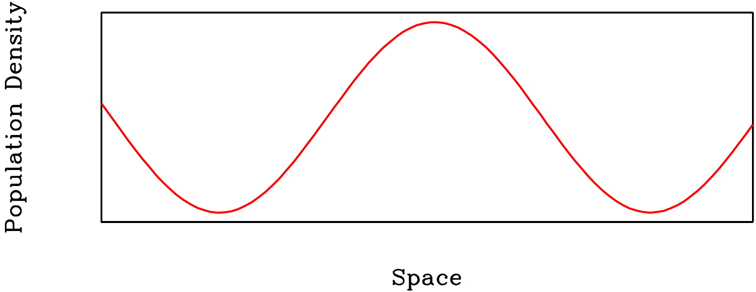

Periodic Travelling Waves in Red Grouse & Field Voles

Spatiotemporal data shows that both red grouse cycles on Kerloch Moor and field vole cycles in Kielder Forest are spatially organised into a periodic travelling wave (wavetrain)

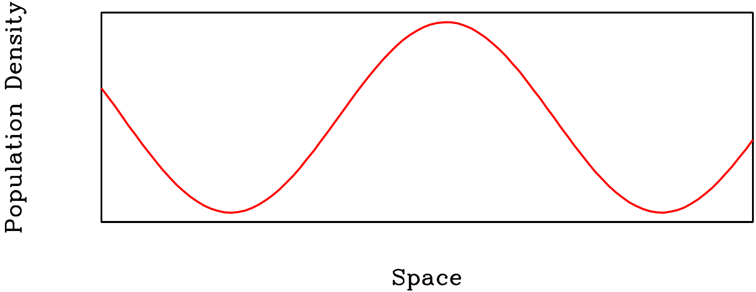

Periodic Travelling Waves in Red Grouse & Field Voles

Spatiotemporal data shows that both red grouse cycles on Kerloch Moor and field vole cycles in Kielder Forest are spatially organised into a periodic travelling wave (wavetrain)

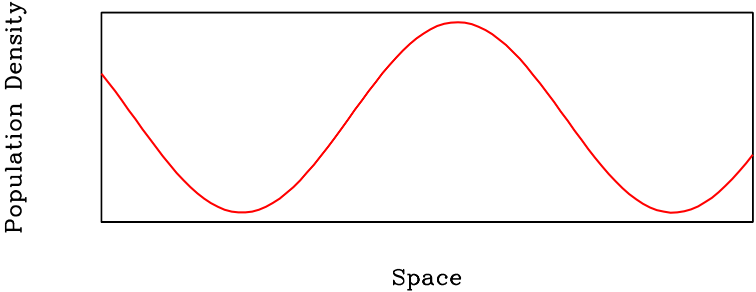

Periodic Travelling Waves in Red Grouse & Field Voles

Spatiotemporal data shows that both red grouse cycles on Kerloch Moor and field vole cycles in Kielder Forest are spatially organised into a periodic travelling wave (wavetrain)

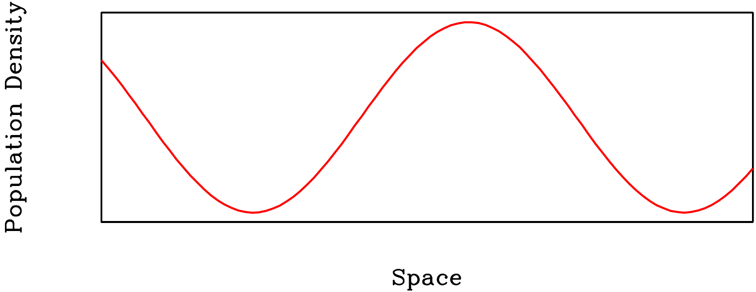

Periodic Travelling Waves in Red Grouse & Field Voles

Spatiotemporal data shows that both red grouse cycles on Kerloch Moor and field vole cycles in Kielder Forest are spatially organised into a periodic travelling wave (wavetrain)

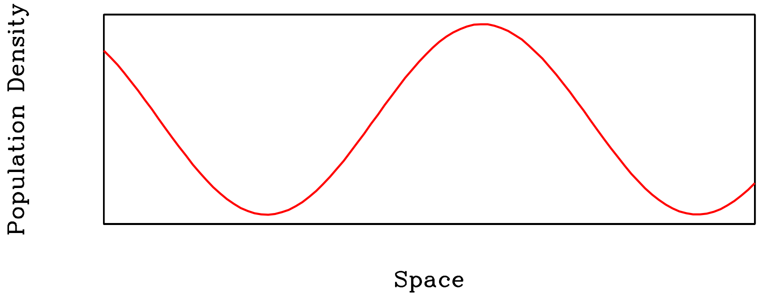

Periodic Travelling Waves in Red Grouse & Field Voles

Spatiotemporal data shows that both red grouse cycles on Kerloch Moor and field vole cycles in Kielder Forest are spatially organised into a periodic travelling wave (wavetrain)

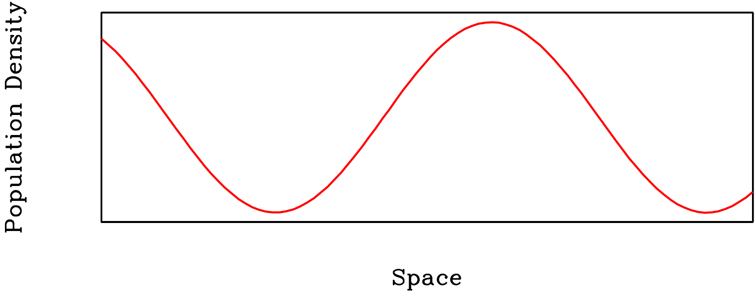

Periodic Travelling Waves in Red Grouse & Field Voles

Spatiotemporal data shows that both red grouse cycles on Kerloch Moor and field vole cycles in Kielder Forest are spatially organised into a periodic travelling wave (wavetrain)

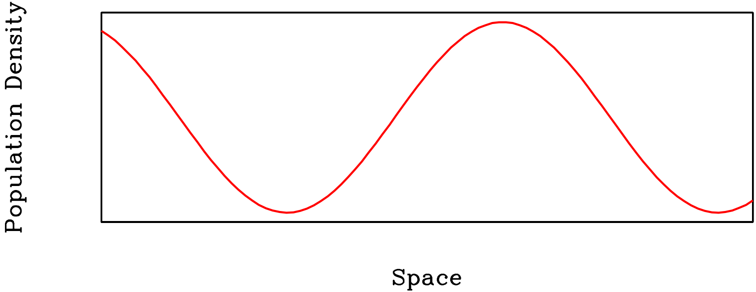

Periodic Travelling Waves in Red Grouse & Field Voles

Spatiotemporal data shows that both red grouse cycles on Kerloch Moor and field vole cycles in Kielder Forest are spatially organised into a periodic travelling wave (wavetrain)

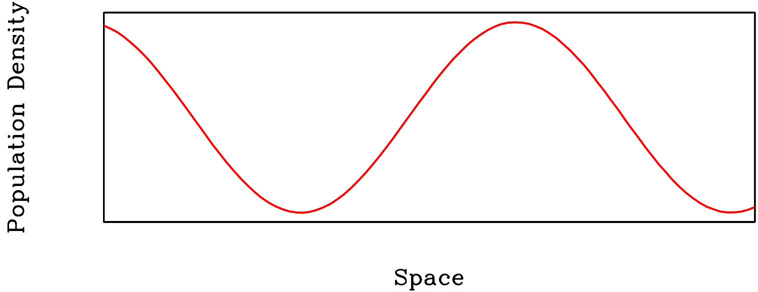

Periodic Travelling Waves in Red Grouse & Field Voles

Spatiotemporal data shows that both red grouse cycles on Kerloch Moor and field vole cycles in Kielder Forest are spatially organised into a periodic travelling wave (wavetrain)

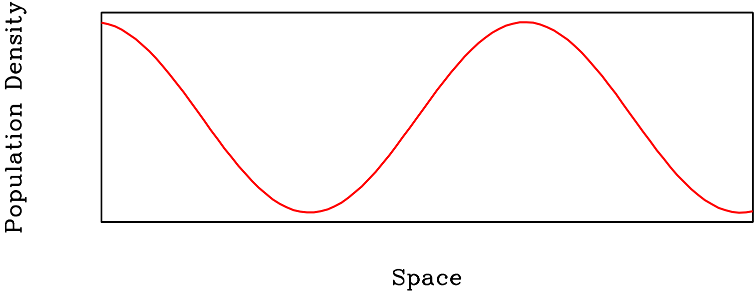

Periodic Travelling Waves in Red Grouse & Field Voles

Spatiotemporal data shows that both red grouse cycles on Kerloch Moor and field vole cycles in Kielder Forest are spatially organised into a periodic travelling wave (wavetrain)

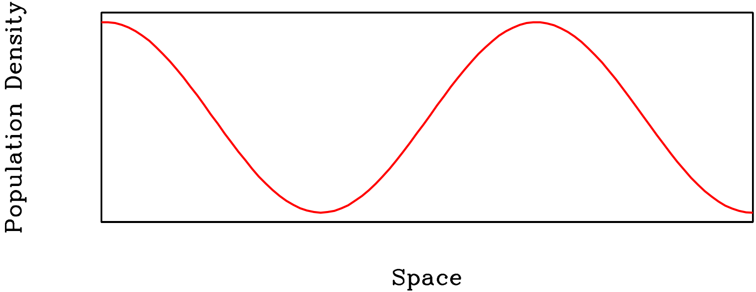

Periodic Travelling Waves in Red Grouse & Field Voles

Spatiotemporal data shows that both red grouse cycles on Kerloch Moor and field vole cycles in Kielder Forest are spatially organised into a periodic travelling wave (wavetrain)

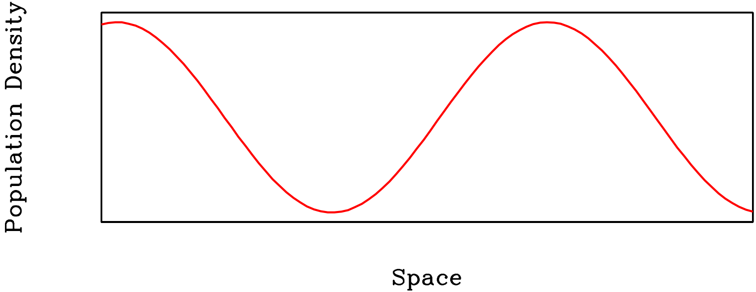

Periodic Travelling Waves in Red Grouse & Field Voles

Spatiotemporal data shows that both red grouse cycles on Kerloch Moor and field vole cycles in Kielder Forest are spatially organised into a periodic travelling wave (wavetrain)

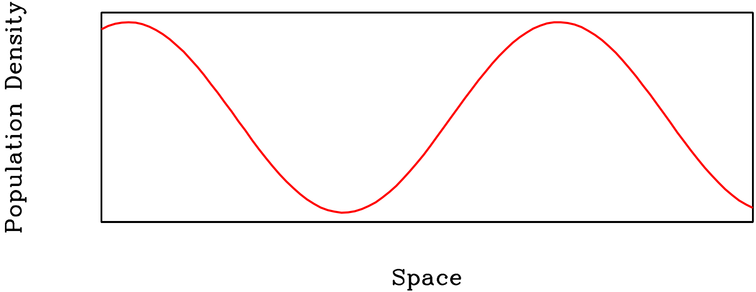

Periodic Travelling Waves in Red Grouse & Field Voles

Spatiotemporal data shows that both red grouse cycles on Kerloch Moor and field vole cycles in Kielder Forest are spatially organised into a periodic travelling wave (wavetrain)

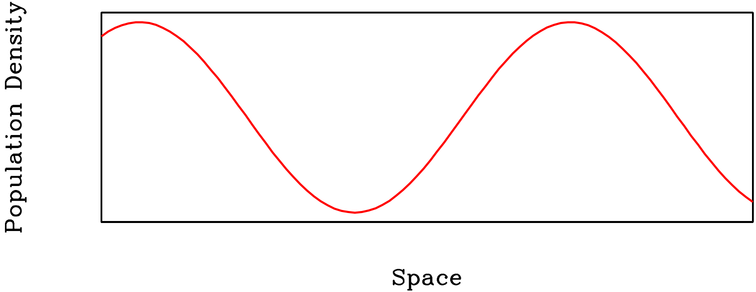

Periodic Travelling Waves in Red Grouse & Field Voles

Spatiotemporal data shows that both red grouse cycles on Kerloch Moor and field vole cycles in Kielder Forest are spatially organised into a periodic travelling wave (wavetrain)

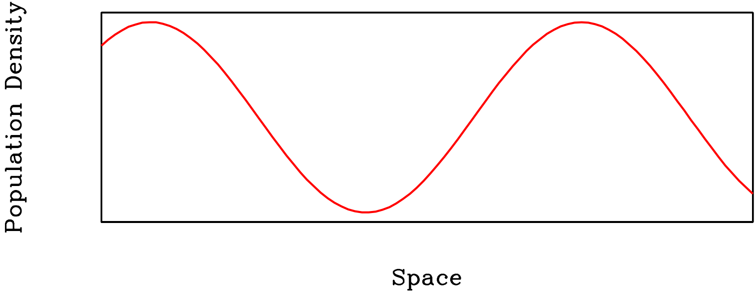

Periodic Travelling Waves in Red Grouse & Field Voles

Spatiotemporal data shows that both red grouse cycles on Kerloch Moor and field vole cycles in Kielder Forest are spatially organised into a periodic travelling wave (wavetrain)

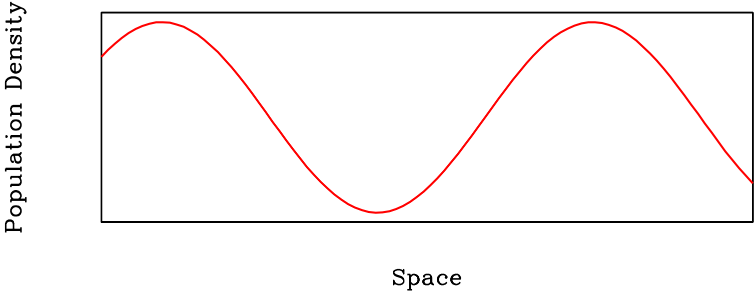

Periodic Travelling Waves in Red Grouse & Field Voles

Spatiotemporal data shows that both red grouse cycles on Kerloch Moor and field vole cycles in Kielder Forest are spatially organised into a periodic travelling wave (wavetrain)

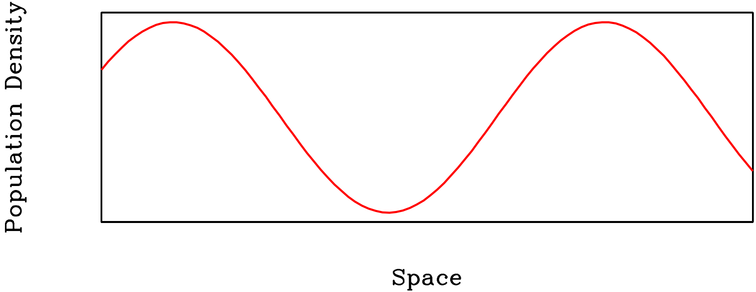

Periodic Travelling Waves in Red Grouse & Field Voles

Spatiotemporal data shows that both red grouse cycles on Kerloch Moor and field vole cycles in Kielder Forest are spatially organised into a periodic travelling wave (wavetrain)

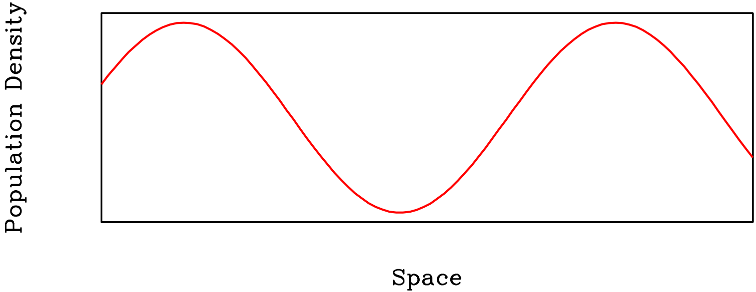

Periodic Travelling Waves in Red Grouse & Field Voles

Spatiotemporal data shows that both red grouse cycles on Kerloch Moor and field vole cycles in Kielder Forest are spatially organised into a periodic travelling wave (wavetrain)

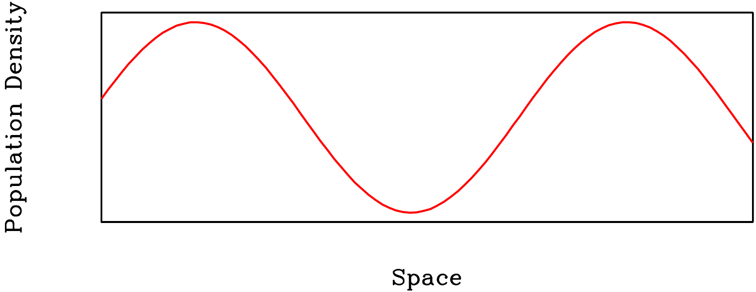

Periodic Travelling Waves in Red Grouse & Field Voles

Spatiotemporal data shows that both red grouse cycles on Kerloch Moor and field vole cycles in Kielder Forest are spatially organised into a periodic travelling wave (wavetrain)

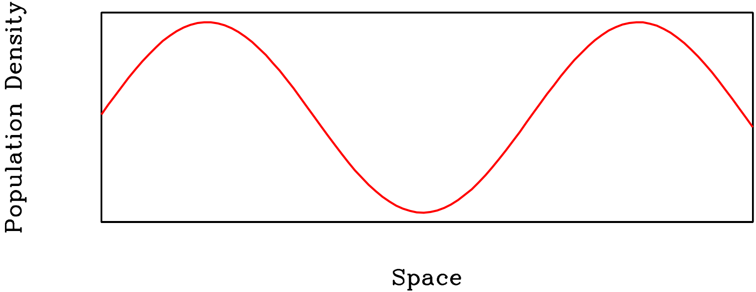

Periodic Travelling Waves in Red Grouse & Field Voles

Spatiotemporal data shows that both red grouse cycles on Kerloch Moor and field vole cycles in Kielder Forest are spatially organised into a periodic travelling wave (wavetrain)

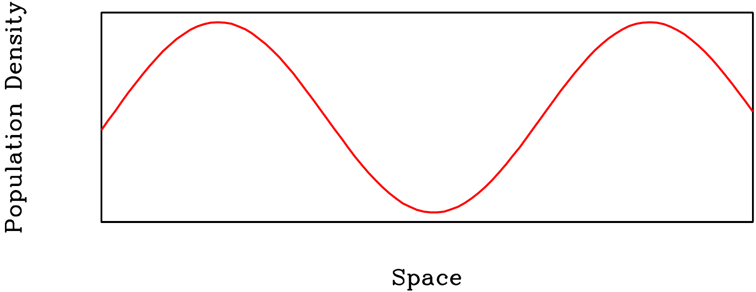

Periodic Travelling Waves in Red Grouse & Field Voles

Spatiotemporal data shows that both red grouse cycles on Kerloch Moor and field vole cycles in Kielder Forest are spatially organised into a periodic travelling wave (wavetrain)

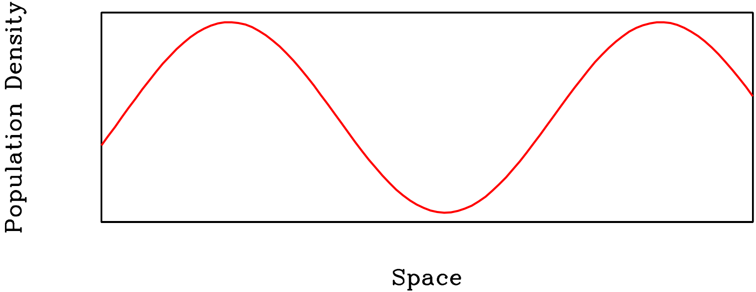

Periodic Travelling Waves in Red Grouse & Field Voles

Spatiotemporal data shows that both red grouse cycles on Kerloch Moor and field vole cycles in Kielder Forest are spatially organised into a periodic travelling wave (wavetrain)

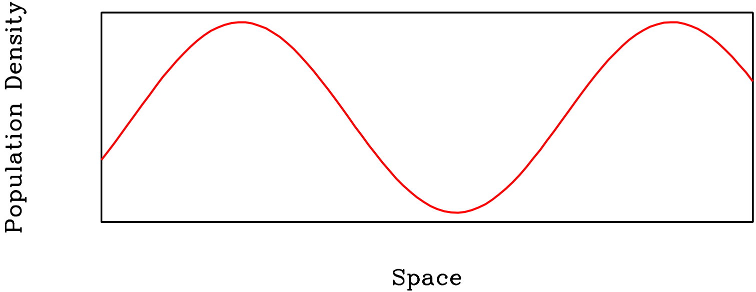

Periodic Travelling Waves in Red Grouse & Field Voles

Spatiotemporal data shows that both red grouse cycles on Kerloch Moor and field vole cycles in Kielder Forest are spatially organised into a periodic travelling wave (wavetrain)

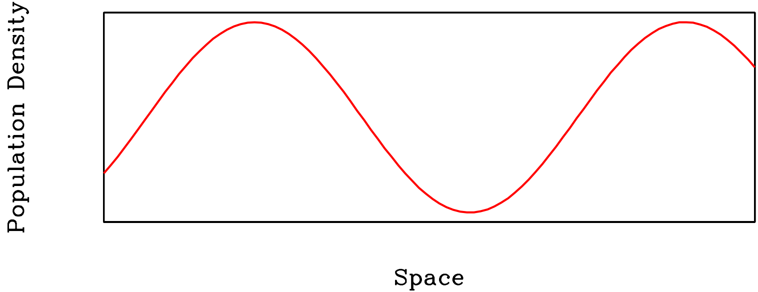

Periodic Travelling Waves in Red Grouse & Field Voles

Spatiotemporal data shows that both red grouse cycles on Kerloch Moor and field vole cycles in Kielder Forest are spatially organised into a periodic travelling wave (wavetrain)

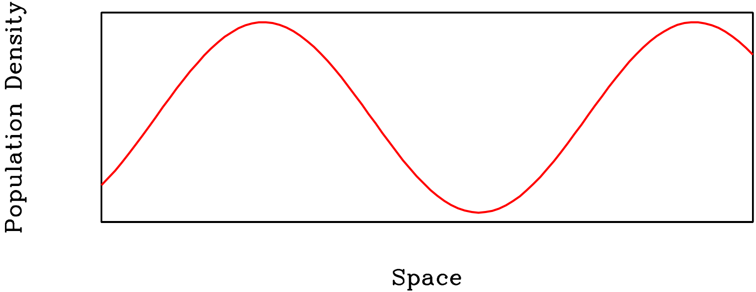

Periodic Travelling Waves in Red Grouse & Field Voles

Spatiotemporal data shows that both red grouse cycles on Kerloch Moor and field vole cycles in Kielder Forest are spatially organised into a periodic travelling wave (wavetrain)

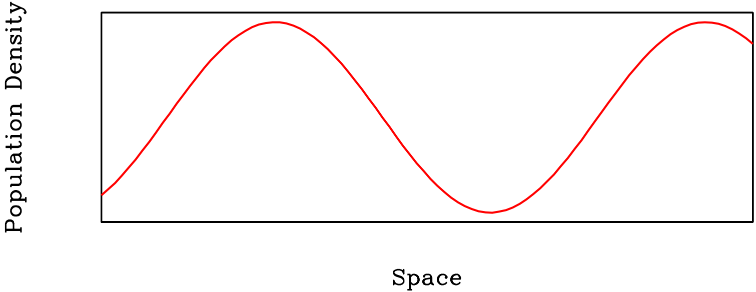

Periodic Travelling Waves in Red Grouse & Field Voles

Spatiotemporal data shows that both red grouse cycles on Kerloch Moor and field vole cycles in Kielder Forest are spatially organised into a periodic travelling wave (wavetrain)

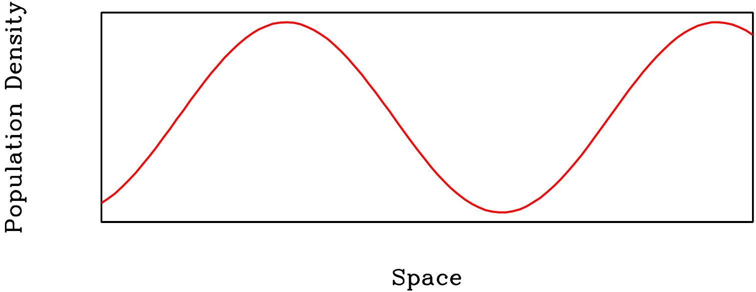

Periodic Travelling Waves in Red Grouse & Field Voles

Spatiotemporal data shows that both red grouse cycles on Kerloch Moor and field vole cycles in Kielder Forest are spatially organised into a periodic travelling wave (wavetrain)

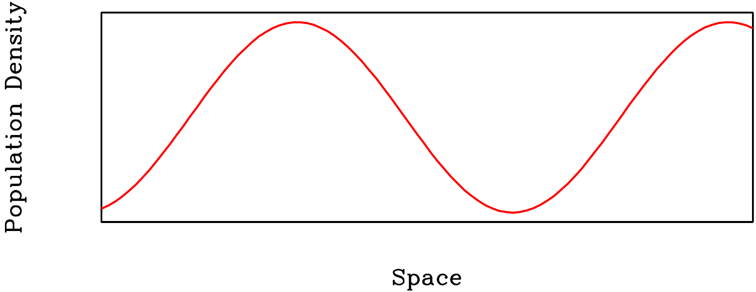

Periodic Travelling Waves in Red Grouse & Field Voles

Spatiotemporal data shows that both red grouse cycles on Kerloch Moor and field vole cycles in Kielder Forest are spatially organised into a periodic travelling wave (wavetrain)

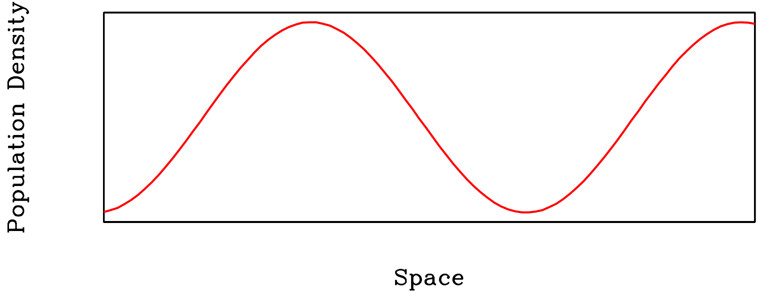

Periodic Travelling Waves in Red Grouse & Field Voles

Spatiotemporal data shows that both red grouse cycles on Kerloch Moor and field vole cycles in Kielder Forest are spatially organised into a periodic travelling wave (wavetrain)

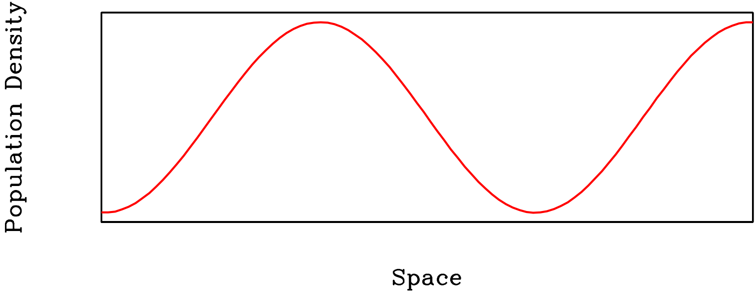

Periodic Travelling Waves in Red Grouse & Field Voles

Spatiotemporal data shows that both red grouse cycles on Kerloch Moor and field vole cycles in Kielder Forest are spatially organised into a periodic travelling wave (wavetrain)

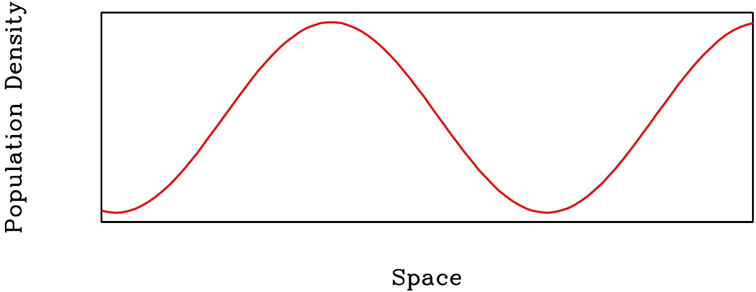

Periodic Travelling Waves in Red Grouse & Field Voles

Spatiotemporal data shows that both red grouse cycles on Kerloch Moor and field vole cycles in Kielder Forest are spatially organised into a periodic travelling wave (wavetrain)

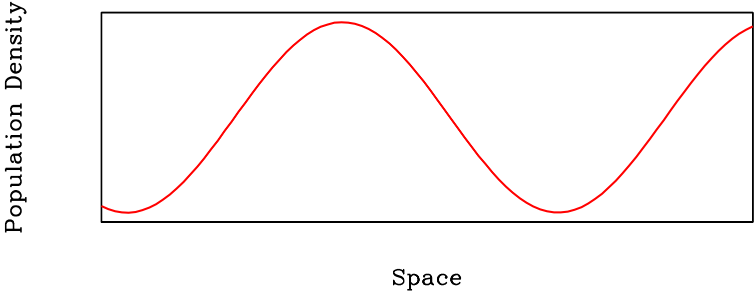

Periodic Travelling Waves in Red Grouse & Field Voles

Spatiotemporal data shows that both red grouse cycles on Kerloch Moor and field vole cycles in Kielder Forest are spatially organised into a periodic travelling wave (wavetrain)

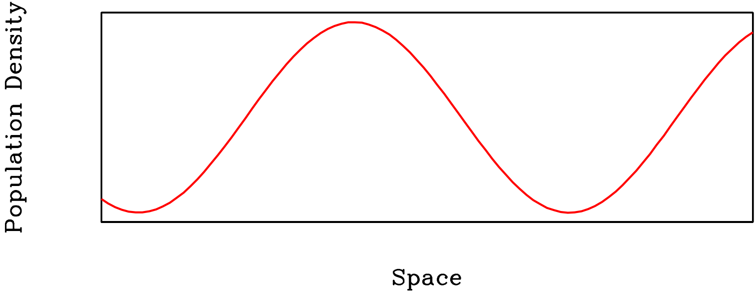

Periodic Travelling Waves in Red Grouse & Field Voles

Spatiotemporal data shows that both red grouse cycles on Kerloch Moor and field vole cycles in Kielder Forest are spatially organised into a periodic travelling wave (wavetrain)

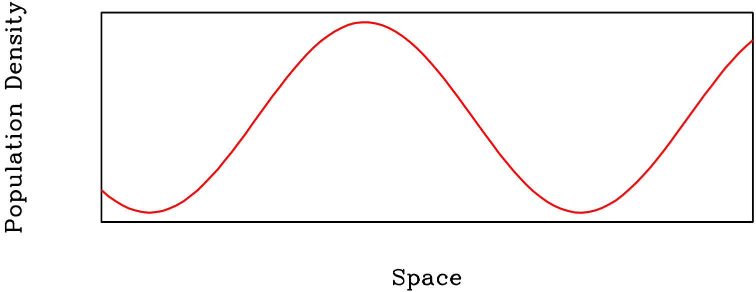

Periodic Travelling Waves in Red Grouse & Field Voles

Spatiotemporal data shows that both red grouse cycles on Kerloch Moor and field vole cycles in Kielder Forest are spatially organised into a periodic travelling wave (wavetrain)

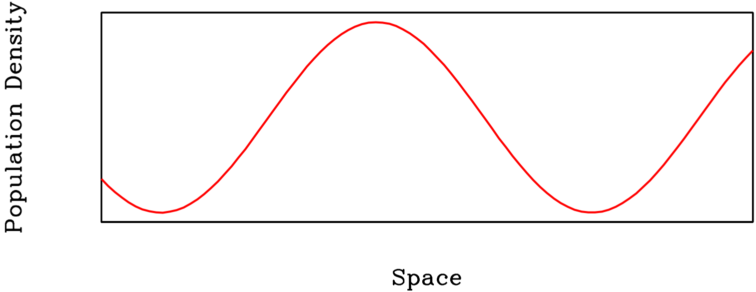

Periodic Travelling Waves in Red Grouse & Field Voles

Spatiotemporal data shows that both red grouse cycles on Kerloch Moor and field vole cycles in Kielder Forest are spatially organised into a periodic travelling wave (wavetrain)

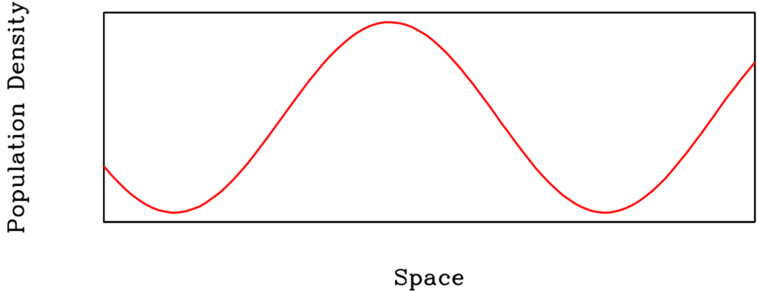

Periodic Travelling Waves in Red Grouse & Field Voles

Spatiotemporal data shows that both red grouse cycles on Kerloch Moor and field vole cycles in Kielder Forest are spatially organised into a periodic travelling wave (wavetrain)

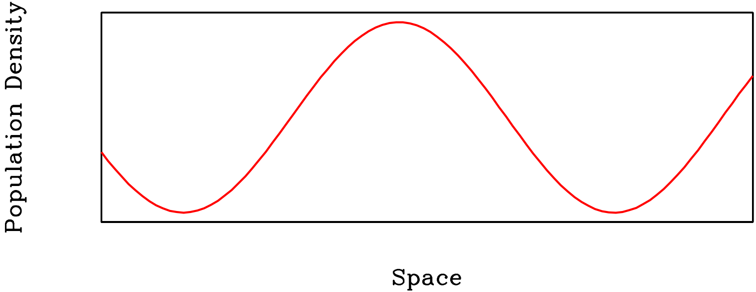

Periodic Travelling Waves in Red Grouse & Field Voles

Spatiotemporal data shows that both red grouse cycles on Kerloch Moor and field vole cycles in Kielder Forest are spatially organised into a periodic travelling wave (wavetrain)

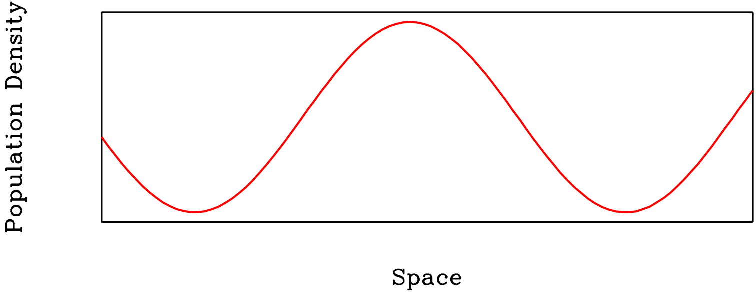

Periodic Travelling Waves in Red Grouse & Field Voles

Spatiotemporal data shows that both red grouse cycles on Kerloch Moor and field vole cycles in Kielder Forest are spatially organised into a periodic travelling wave (wavetrain)

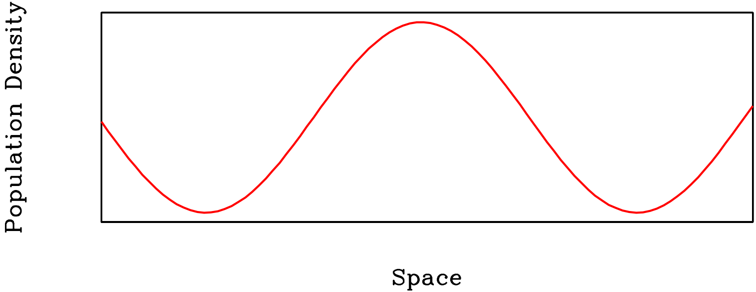

Periodic Travelling Waves in Red Grouse & Field Voles

Spatiotemporal data shows that both red grouse cycles on Kerloch Moor and field vole cycles in Kielder Forest are spatially organised into a periodic travelling wave (wavetrain)

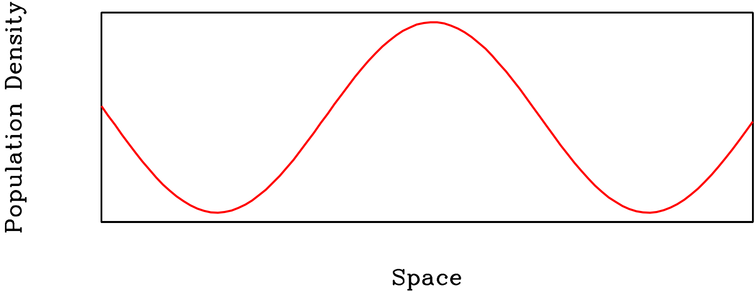

Periodic Travelling Waves in Red Grouse & Field Voles

Spatiotemporal data shows that both red grouse cycles on Kerloch Moor and field vole cycles in Kielder Forest are spatially organised into a periodic travelling wave (wavetrain)

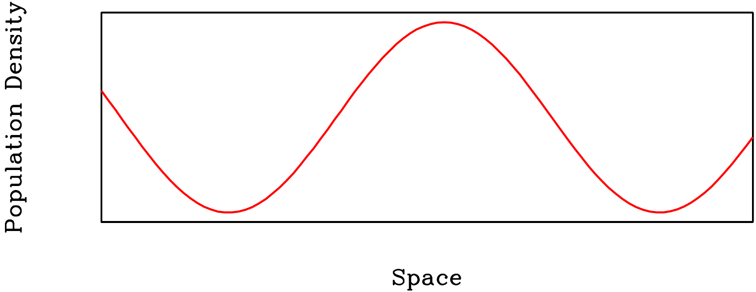

Periodic Travelling Waves in Red Grouse & Field Voles

Spatiotemporal data shows that both red grouse cycles on Kerloch Moor and field vole cycles in Kielder Forest are spatially organised into a periodic travelling wave (wavetrain)

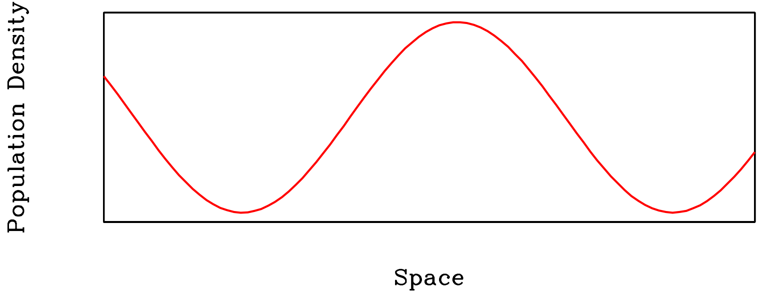

Periodic Travelling Waves in Red Grouse & Field Voles

Spatiotemporal data shows that both red grouse cycles on Kerloch Moor and field vole cycles in Kielder Forest are spatially organised into a periodic travelling wave (wavetrain)

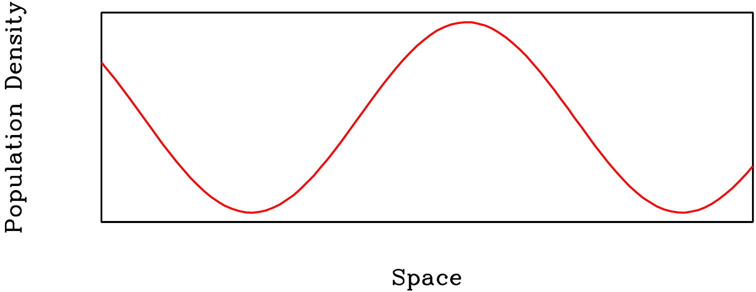

Periodic Travelling Waves in Red Grouse & Field Voles

Spatiotemporal data shows that both red grouse cycles on Kerloch Moor and field vole cycles in Kielder Forest are spatially organised into a periodic travelling wave (wavetrain)

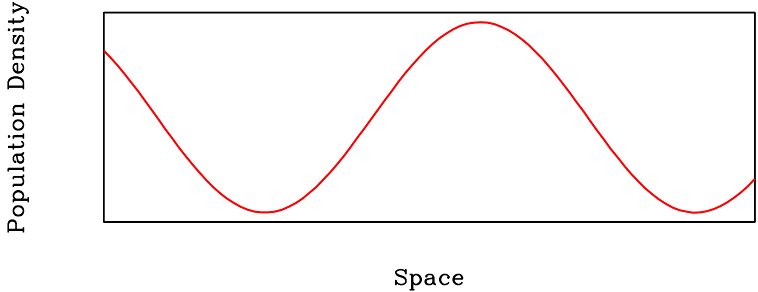

Periodic Travelling Waves in Red Grouse & Field Voles

Spatiotemporal data shows that both red grouse cycles on Kerloch Moor and field vole cycles in Kielder Forest are spatially organised into a periodic travelling wave (wavetrain)

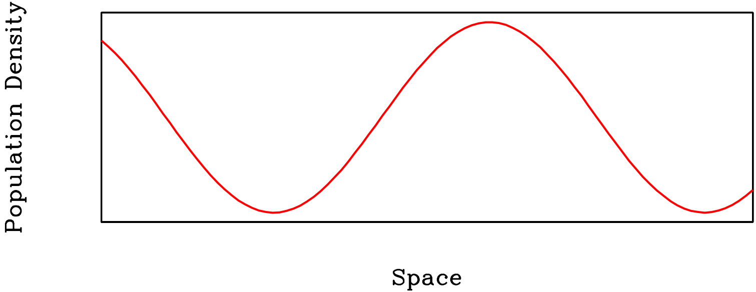

Periodic Travelling Waves in Red Grouse & Field Voles

Spatiotemporal data shows that both red grouse cycles on Kerloch Moor and field vole cycles in Kielder Forest are spatially organised into a periodic travelling wave (wavetrain)

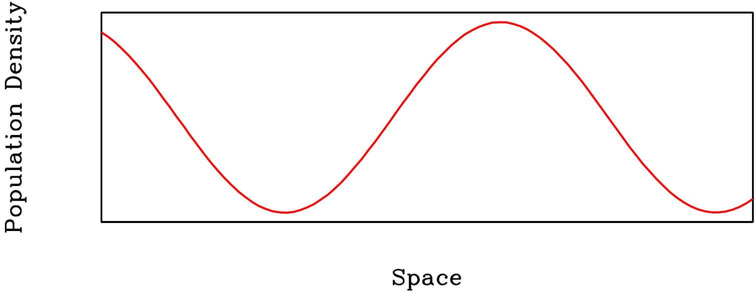

Periodic Travelling Waves in Red Grouse & Field Voles

Spatiotemporal data shows that both red grouse cycles on Kerloch Moor and field vole cycles in Kielder Forest are spatially organised into a periodic travelling wave (wavetrain)

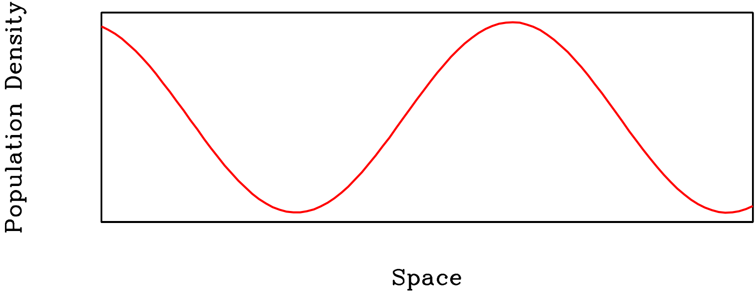

Periodic Travelling Waves in Red Grouse & Field Voles

Spatiotemporal data shows that both red grouse cycles on Kerloch Moor and field vole cycles in Kielder Forest are spatially organised into a periodic travelling wave (wavetrain)

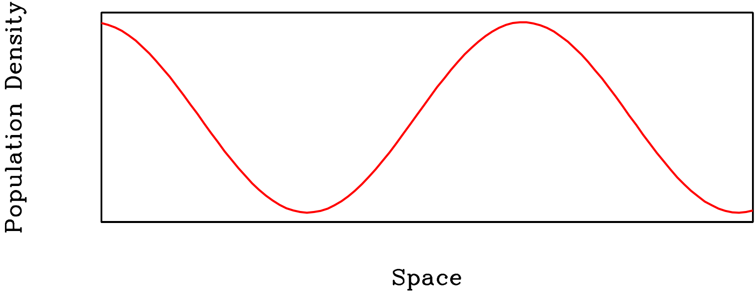

Periodic Travelling Waves in Red Grouse & Field Voles

Spatiotemporal data shows that both red grouse cycles on Kerloch Moor and field vole cycles in Kielder Forest are spatially organised into a periodic travelling wave (wavetrain)

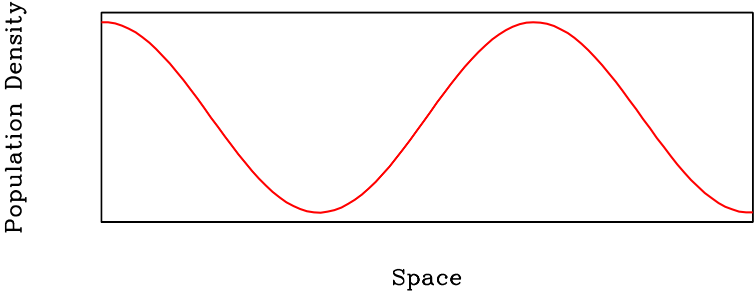

Periodic Travelling Waves in Red Grouse & Field Voles

Spatiotemporal data shows that both red grouse cycles on Kerloch Moor and field vole cycles in Kielder Forest are spatially organised into a periodic travelling wave (wavetrain)

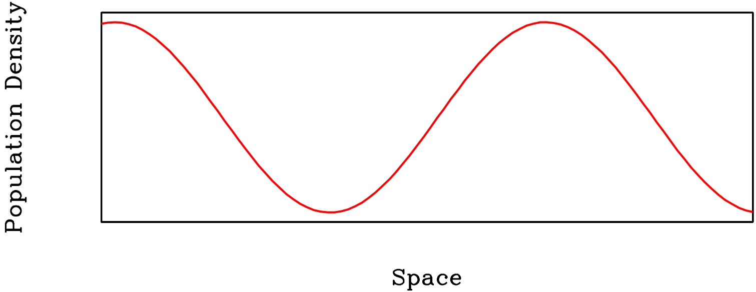

Periodic Travelling Waves in Red Grouse & Field Voles

Spatiotemporal data shows that both red grouse cycles on Kerloch Moor and field vole cycles in Kielder Forest are spatially organised into a periodic travelling wave (wavetrain)

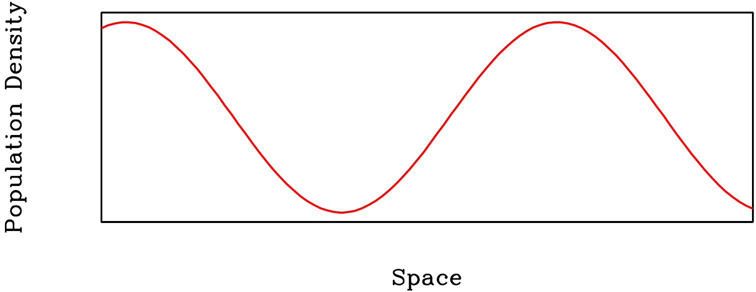

Periodic Travelling Waves in Red Grouse & Field Voles

Spatiotemporal data shows that both red grouse cycles on Kerloch Moor and field vole cycles in Kielder Forest are spatially organised into a periodic travelling wave (wavetrain)

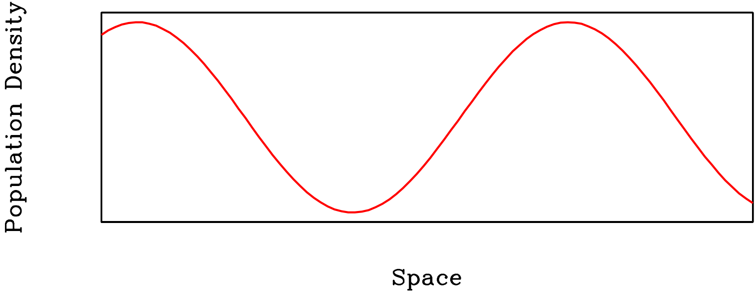

Periodic Travelling Waves in Red Grouse & Field Voles

Spatiotemporal data shows that both red grouse cycles on Kerloch Moor and field vole cycles in Kielder Forest are spatially organised into a periodic travelling wave (wavetrain)

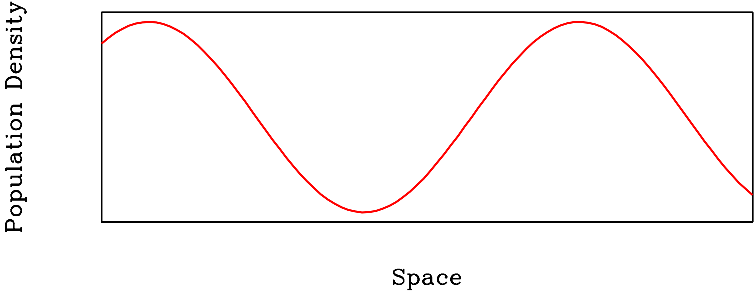

Periodic Travelling Waves in Red Grouse & Field Voles

Spatiotemporal data shows that both red grouse cycles on Kerloch Moor and field vole cycles in Kielder Forest are spatially organised into a periodic travelling wave (wavetrain)

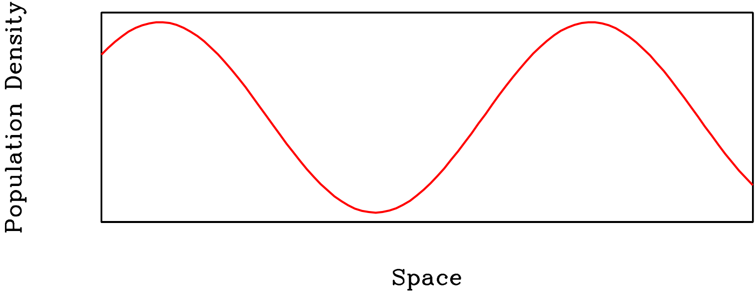

Periodic Travelling Waves in Red Grouse & Field Voles

Spatiotemporal data shows that both red grouse cycles on Kerloch Moor and field vole cycles in Kielder Forest are spatially organised into a periodic travelling wave (wavetrain)

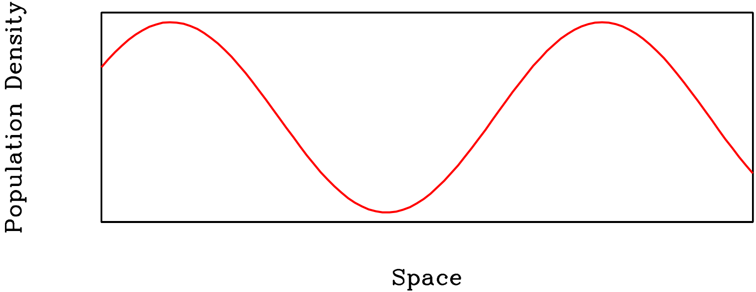

Periodic Travelling Waves in Red Grouse & Field Voles

Spatiotemporal data shows that both red grouse cycles on Kerloch Moor and field vole cycles in Kielder Forest are spatially organised into a periodic travelling wave (wavetrain)

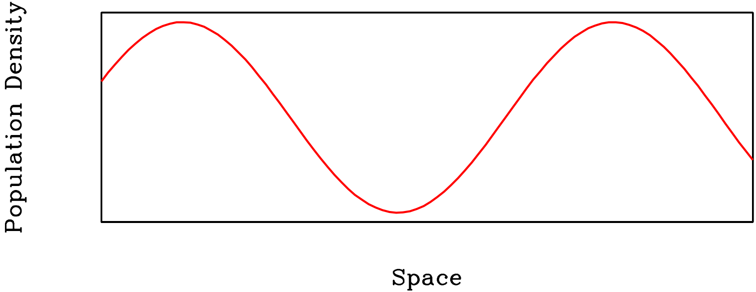

Periodic Travelling Waves in Red Grouse & Field Voles

Spatiotemporal data shows that both red grouse cycles on Kerloch Moor and field vole cycles in Kielder Forest are spatially organised into a periodic travelling wave (wavetrain)

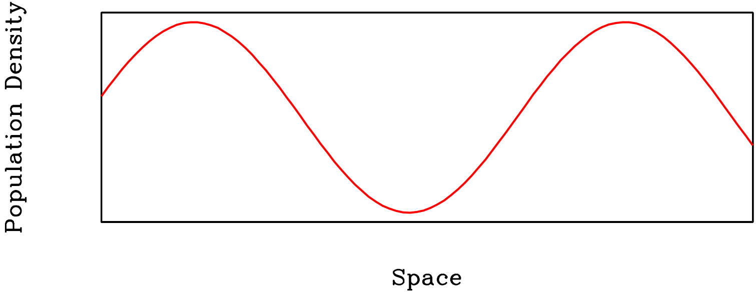

Periodic Travelling Waves in Red Grouse & Field Voles

Spatiotemporal data shows that both red grouse cycles on Kerloch Moor and field vole cycles in Kielder Forest are spatially organised into a periodic travelling wave (wavetrain)

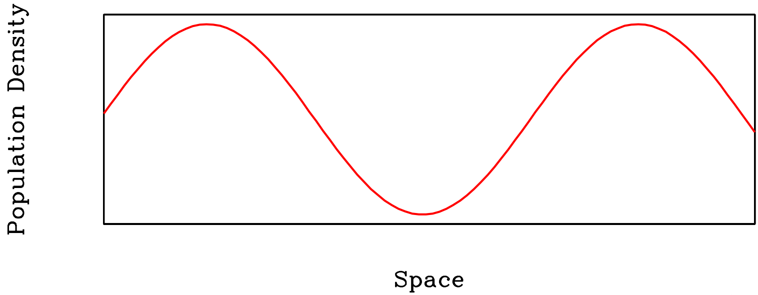

Periodic Travelling Waves in Red Grouse & Field Voles

Spatiotemporal data shows that both red grouse cycles on Kerloch Moor and field vole cycles in Kielder Forest are spatially organised into a periodic travelling wave (wavetrain)

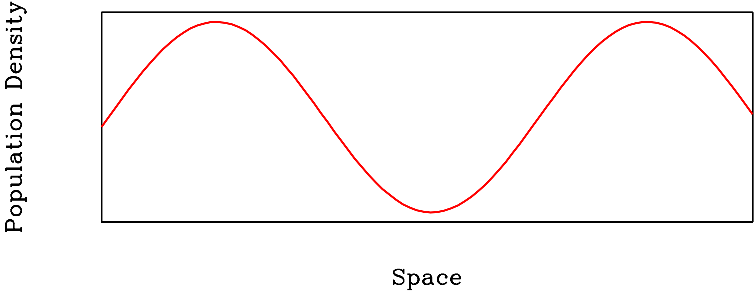

Periodic Travelling Waves in Red Grouse & Field Voles

Spatiotemporal data shows that both red grouse cycles on Kerloch Moor and field vole cycles in Kielder Forest are spatially organised into a periodic travelling wave (wavetrain)

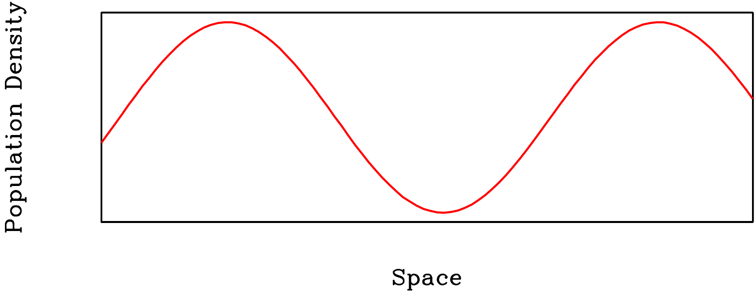

Periodic Travelling Waves in Red Grouse & Field Voles

Spatiotemporal data shows that both red grouse cycles on Kerloch Moor and field vole cycles in Kielder Forest are spatially organised into a periodic travelling wave (wavetrain)

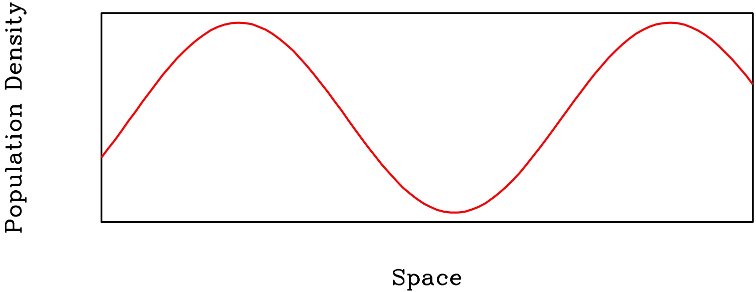

Periodic Travelling Wave Generation Question

Question

Does the Dirichlet condition at the habitat boundary play a role in generating the periodic travelling waves?

Outline

Mathematical Model

I consider a generic oscillator model ("λ–ω equations")

$$\begin{aligned}
\frac{\partial u}{\partial t} &= \frac{\partial^2 u}{\partial x^2} + \lambda(r)u - \omega(r)v \\
\frac{\partial v}{\partial t} &= \frac{\partial^2 v}{\partial x^2} + \omega(r)u + \lambda(r)v \\
r &= \sqrt{u^2 + v^2} \\
\lambda(r) &= 1 - r^2 \\
\omega(r) &= \omega_0 + \omega_1 r^2
\end{aligned}$$

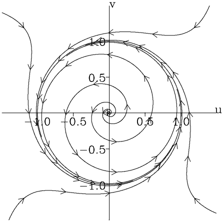

This is the normal form of an oscillatory reaction-diffusion system with scalar diffusion close to a supercritical Hopf bifurcation

Typical Model Solutions

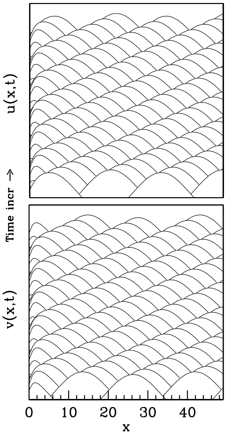

Eqns:
$$\begin{aligned}
\frac{\partial u}{\partial t} &= \frac{\partial^2 u}{\partial x^2} + \lambda(r)u - \omega(r)v \\
\frac{\partial v}{\partial t} &= \frac{\partial^2 v}{\partial x^2} + \omega(r)u + \lambda(r)v \\
r &= \sqrt{u^2 + v^2} \\
\lambda(r) &= 1 - r^2 \\
\omega(r) &= \omega_0 + \omega_1 r^2
\end{aligned}$$

Bcs:
$$\begin{aligned}
u = v = 0 \quad &\text{at} \quad x = 0 \\
u_x = v_x = 0 \quad &\text{at} \quad x = 50
\end{aligned}$$

Typical Model Solutions

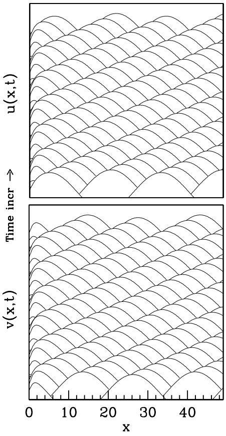

Conclusion

Dirichlet boundary conditions generate a periodic travelling wave

Question

What is the amplitude, speed and wavelength of the periodic travelling wave?

Amplitude and Phase Equations

To study the λ–ω equations, it is helpful to replace u and v by $r = \sqrt{u^2 + v^2}$ and $\theta = \tan^{-1}(v/u)$, giving

$$\begin{aligned} r_t &= r_{xx} - r\theta_x^2 + r(1 - r^2) \\ \theta_t &= \theta_{xx} + \frac{2r_x\theta_x}{r} + \omega_0 - \omega_1 r^2 \end{aligned}$$

Family of periodic travelling wave solutions ($0 < r^* < 1$):

$$\left\{ \begin{array}{l} r = r^* \\ \theta = \left[\omega(r^*)t \pm \sqrt{\lambda(r^*)}x\right] \end{array} \right\} \leftrightarrow \left\{ \begin{array}{l} u = r^* \cos\left[\omega(r^*)t \pm \sqrt{\lambda(r^*)}x\right] \\ v = r^* \sin\left[\omega(r^*)t \pm \sqrt{\lambda(r^*)}x\right] \end{array} \right\}$$

Our question: what r^* is selected by the Dirichlet boundary condition?

Typical Solutions Replotted

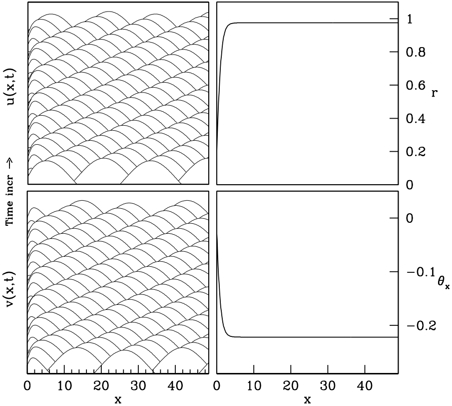

Replotting the solutions in terms of r and θ_x shows that the long-term solutions for r and θ_x are independent of time

Equilibrium Equations and the Wavetrain Amplitude

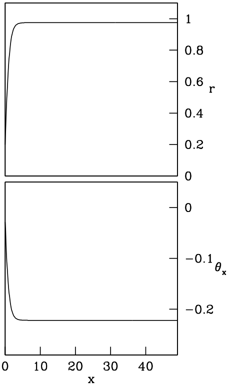

There is an exact solution for
$r = R(x)$, $\theta_x = \Psi(x)$ on $0 < x < \infty$:

$$R(x) = R^* \tanh\left(x/\sqrt{2}\right) \qquad \Psi(x) = \Psi^* \tanh\left(x/\sqrt{2}\right)$$

$$R^* = \left\{\tfrac{1}{2}\left[1+\sqrt{1+\tfrac{8}{9}\omega_1^2}\right]\right\}^{-1/2} \quad \Psi^* = -\mathrm{sign}(\omega_1)\left(1-{R^*}^2\right)^{1/2}$$

Equilibrium Equations and the Wavetrain Amplitude

Wave amplitude R^* is in very good agreement with that found in numerical simulations.

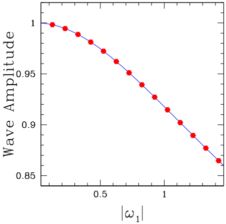

There is an exact solution for $r = R(x)$, $\theta_x = \Psi(x)$ on $0 < x < \infty$:

$$R(x) = R^* \tanh\left(x/\sqrt{2}\right) \qquad \Psi(x) = \Psi^* \tanh\left(x/\sqrt{2}\right)$$

$$R^* = \left\{\tfrac{1}{2}\left[1+\sqrt{1+\tfrac{8}{9}\omega_1^2}\right]\right\}^{-1/2} \qquad \Psi^* = -\mathrm{sign}(\omega_1)\left(1-R^{*\,2}\right)^{1/2}$$

Outline

1. Ecological Motivation
2. A Generic Mathematical Model
3. **Periodic Travelling Wave Stability**
4. Source-Sink Dynamics
5. Conclusions

Stability in the Periodic Travelling Wave Family

In any oscillatory reaction-diffusion system, some members of the periodic travelling wave family are stable as solutions of the partial differential equations, while others are unstable.

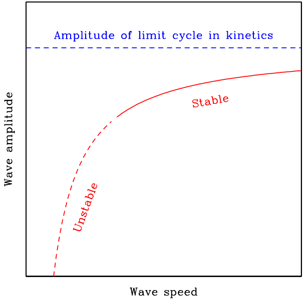

For our λ–ω system, the stability condition is

$$r^* > \left(\frac{2 + 2\omega_1^2}{3 + 2\omega_1^2} \right)^{1/2}$$

Stability of the Selected Wave

The stability of the selected wave depends on ω_1.

$$R^* = \left\{ \tfrac{1}{2} \left[1 + \sqrt{1 + \tfrac{8}{9}\omega_1^2} \right] \right\}^{-1/2}$$

This is stable

$$\Leftrightarrow \quad R^* > \left(\frac{2 + 2\omega_1^2}{3 + 2\omega_1^2} \right)^{1/2}$$

$$\Leftrightarrow \quad |\omega_1| < 1.110468\ldots$$

Stability of the Selected Wave

The stability of the selected wave depends on ω_1.

$$R^* = \left\{ \frac{1}{2} \left[1 + \sqrt{1 + \frac{8}{9}\omega_1^2} \right] \right\}^{-1/2}$$

This is stable

$$\Leftrightarrow \quad R^* > \left(\frac{2 + 2\omega_1^2}{3 + 2\omega_1^2} \right)^{1/2}$$

$$\Leftrightarrow \quad |\omega_1| < 1.110468\ldots$$

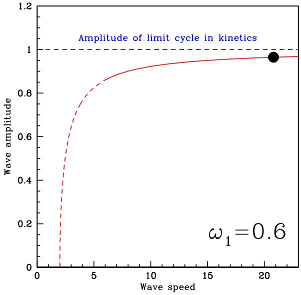

Stability of the Selected Wave

The stability of the selected wave depends on ω_1.

$$R^* = \left\{ \frac{1}{2} \left[1 + \sqrt{1 + \frac{8}{9}\omega_1^2} \right] \right\}^{-1/2}$$

This is stable

$$\Leftrightarrow \quad R^* > \left(\frac{2 + 2\omega_1^2}{3 + 2\omega_1^2} \right)^{1/2}$$

$$\Leftrightarrow \quad |\omega_1| < 1.110468\ldots$$

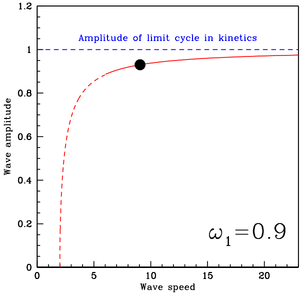

Stability of the Selected Wave

The stability of the selected wave depends on ω_1.

$$R^* = \left\{ \frac{1}{2} \left[1 + \sqrt{1 + \frac{8}{9}\omega_1^2} \right] \right\}^{-1/2}$$

This is stable

$$\Leftrightarrow \quad R^* > \left(\frac{2 + 2\omega_1^2}{3 + 2\omega_1^2} \right)^{1/2}$$

$$\Leftrightarrow \quad |\omega_1| < 1.110468\ldots$$

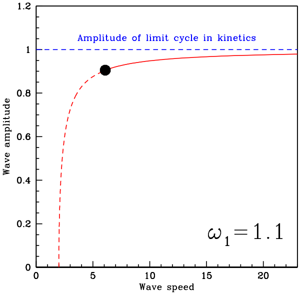

Stability of the Selected Wave

The stability of the selected wave depends on ω_1.

$$R^* = \left\{ \frac{1}{2} \left[1 + \sqrt{1 + \frac{8}{9}\omega_1^2} \right] \right\}^{-1/2}$$

This is stable

$$\Leftrightarrow \quad R^* > \left(\frac{2 + 2\omega_1^2}{3 + 2\omega_1^2} \right)^{1/2}$$

$$\Leftrightarrow \quad |\omega_1| < 1.110468\ldots$$

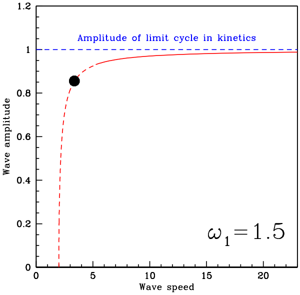

Typical Solution in an Unstable Case

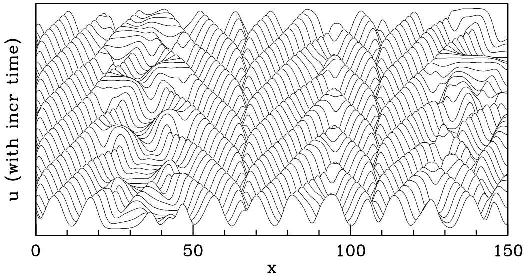

Convective and Absolute Stability

- There are a variety of different solution forms for $|\omega_1| > 1.110468\ldots$ (unstable waves).

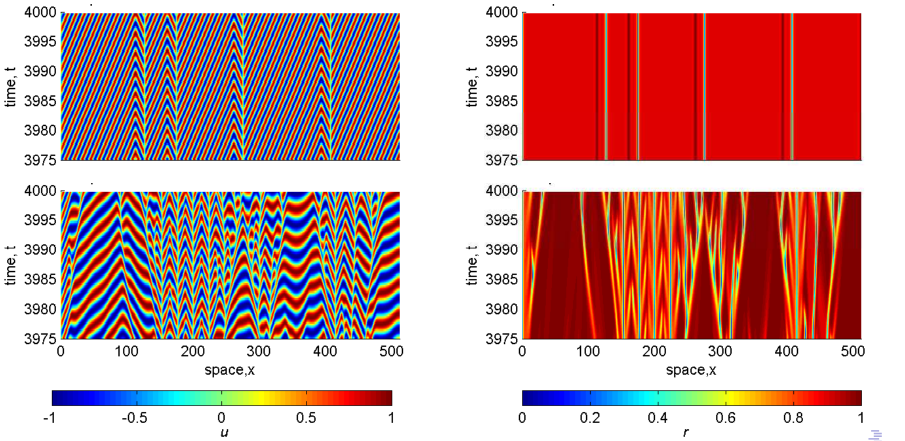

Convective and Absolute Stability

- There are a variety of different solution forms for $|\omega_1| > 1.110468\ldots$ (unstable waves).
- The key concept for distinguishing these is "absolute stability".
- In spatially extended systems, a solution can be unstable, but with any perturbation that grows also moving. This is "convective instability".

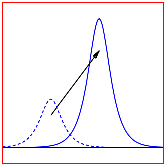

Convective and Absolute Stability

- There are a variety of different solution forms for $|\omega_1| > 1.110468\ldots$ (unstable waves).
- The key concept for distinguishing these is "absolute stability".
- In spatially extended systems, a solution can be unstable, but with any perturbation that grows also moving. This is "convective instability".
- Alternatively, a solution can be unstable with perturbations growing without moving. This is "absolute instability".

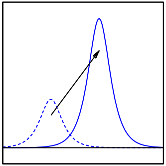

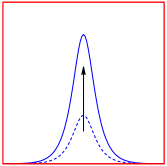

Convective and Absolute Stability

- There are a variety of different solution forms for $|\omega_1| > 1.110468\ldots$ (unstable waves).
- The key concept for distinguishing these is "absolute stability".
- In spatially extended systems, a solution can be unstable, but with any perturbation that grows also moving. This is "convective instability".
- Alternatively, a solution can be unstable with perturbations growing without moving. This is "absolute instability".
- Absolute instability implies instability irrespective of boundary conditions.

Absolute Stability of Wavetrains

- Absolute stability is much harder to calculate than stability.
- For wavetrain solutions of λ–ω reaction-diffusion equations, we have calculated absolute stability by computing the "absolute spectrum" via numerical continuation, adapting the method of Rademacher, Sandstede & Scheel (Physica D 229: 166-183, 2007)

Absolute Stability of Wavetrains

- Absolute stability is much harder to calculate than stability.
- For wavetrain solutions of λ–ω reaction-diffusion equations, we have calculated absolute stability by computing the "absolute spectrum" via numerical continuation, adapting the method of Rademacher, Sandstede & Scheel (Physica D 229: 166-183, 2007)
- Our calculation shows that the stability of the selected wavetrain is:

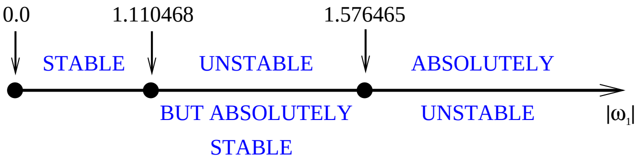

Generation of Absolutely Stable and Unstable Wavetrains by Dirichlet Boundary Conditions

Numerical simulations show distinct behaviours in the absolutely stable and unstable parameter regimes

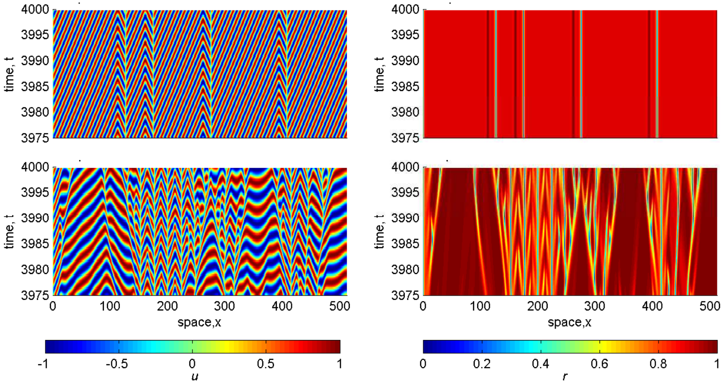

Convectively unstable, absolutely stable

Absolutely unstable

Outline

Sources, Sinks, and Convective Instability

I focus on the convectively unstable but absolutely stable case.

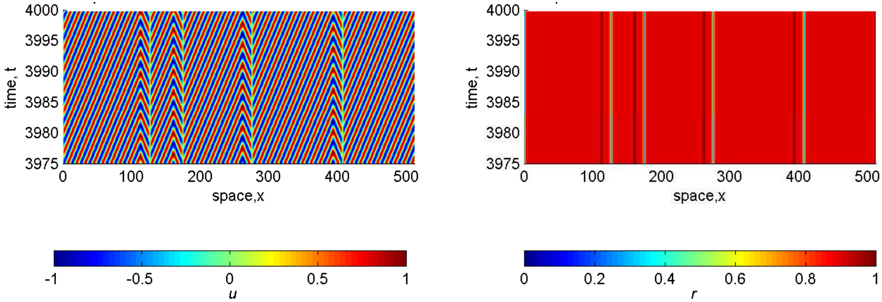

This solution is a pattern of “sources and sinks”.

Sources, Sinks, and Convective Instability

I focus on the convectively unstable but absolutely stable case.

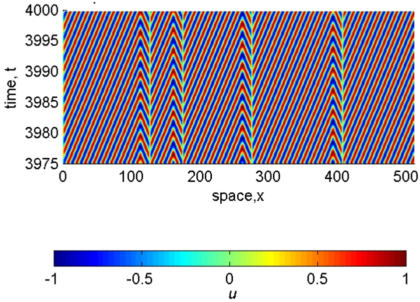

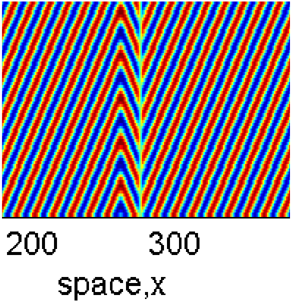

This solution is a pattern of “sources and sinks”.

Sources, Sinks, and Convective Instability

I focus on the convectively unstable but absolutely stable case.

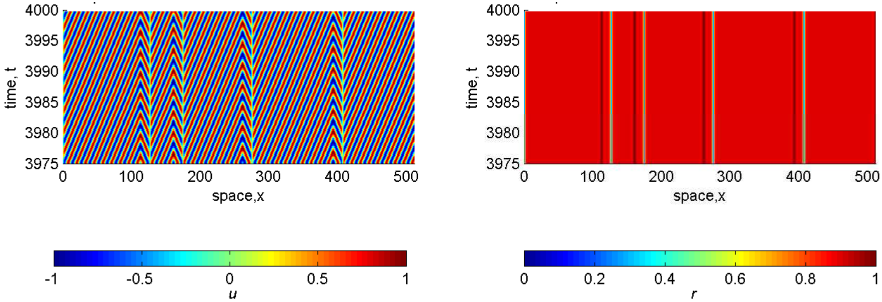

This solution is a pattern of “sources and sinks”.
The wavetrain between the defects has (approximately) amplitude

$$R^* = \left\{ \tfrac{1}{2} \left[1 + \sqrt{1 + \tfrac{8}{9}\omega_1^2} \right] \right\}^{-1/2}.$$

Sources, Sinks, and Convective Instability

Question: How can an unstable wavetrain persist between the sources and sinks?

Sources, Sinks, and Convective Instability

Question: How can an unstable wavetrain persist between the sources and sinks?

Answer: Any growing perturbations moves, and is absorbed when it reaches a sink.

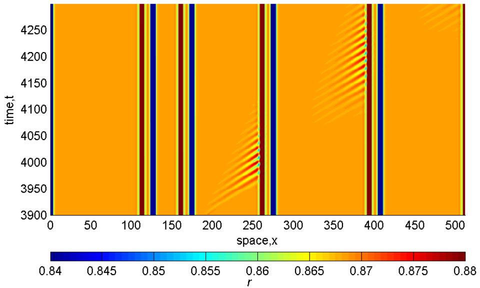

Movement of Sources and Sinks

The sources and sinks appear to be stationary........

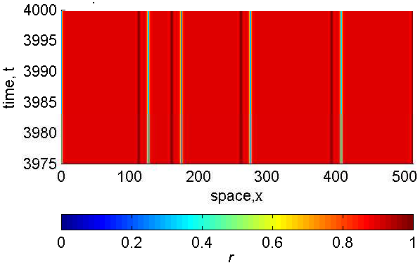

Movement of Sources and Sinks

The sources and sinks appear to be stationary........

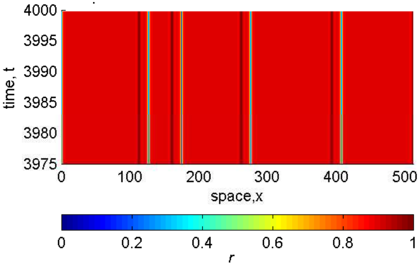

..........but very long simulations show that they move.

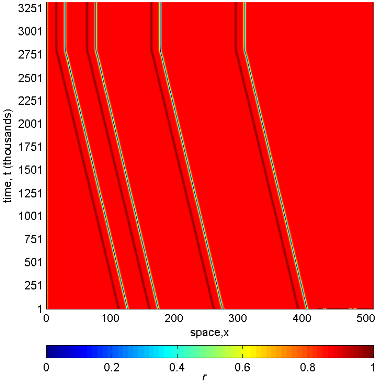

Travelling Waves of Amplitude

The source-sink patterns are of travelling wave form in amplitude.

Substitute $r(x,t)=\widehat{r}(z)$, $\theta_x(x,t)=\widehat{\psi}(z)$, $z=x-ct$

$$\begin{aligned} \Longrightarrow \quad d^2\widehat{r}/dz^2 + c\,d\widehat{r}/dz + \widehat{r}\left(1-\widehat{r}^{\,2}-\widehat{\psi}^{\,2}\right) &= 0 \\ d\widehat{\psi}/dz + c\,\widehat{\psi} + K - \omega_1\widehat{r}^{\,2} + 2\widehat{\psi}\,(d\widehat{r}/dz)/\widehat{r} &= 0 \end{aligned}$$

(K is a constant of integration).

Solution Structure

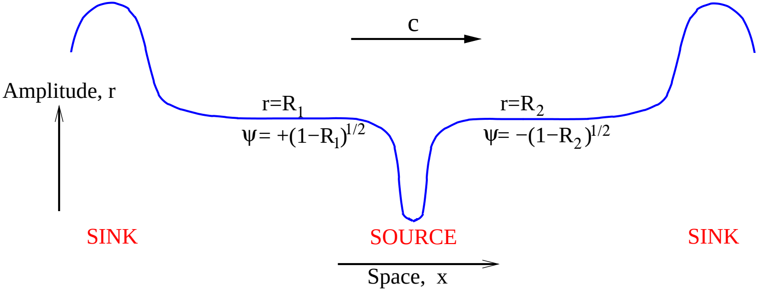

Between the source and the neighbouring sinks,

$$-c(1-R_1^2)^{1/2}+\omega_1 R_1^2 = K = +c(1-R_2^2)^{1/2}+\omega_1 R_2^2$$

$\Longrightarrow$ c has the same sign as $R_1 - R_2$.

Eigenvalue Structure of Stationary Sources and Sinks

Stationary sources and sinks satisfy

$$
\begin{aligned}
d^2\widehat{r}/dz^2 + \widehat{r}\left(1 - \widehat{r}^{\,2} - \widehat{\psi}^{\,2}\right) &= 0 \\
d\widehat{\psi}/dz + K - \omega_1\widehat{r}^{\,2} + 2\widehat{\psi}\,(d\widehat{r}/dz)/\widehat{r} &= 0.
\end{aligned}
$$

Eigenvalue Structure of Stationary Sources and Sinks

Stationary sources and sinks satisfy

$$
\begin{aligned}
d^2\widehat{r}/dz^2 + \widehat{r}\left(1 - \widehat{r}^{\,2} - \widehat{\psi}^{\,2}\right) &= 0 \\
d\widehat{\psi}/dz + K - \omega_1\widehat{r}^{\,2} + 2\widehat{\psi}\,(d\widehat{r}/dz)/\widehat{r} &= 0.
\end{aligned}
$$

Linearise about the wavetrain

$\Rightarrow$ stationary sources decay to the wavetrain at rate $\sqrt{2}$
& stationary sinks decay to the wavetrain at rate $1/\sqrt{2} \pm i\delta/4$

$(\delta = \sqrt{11 - 12R^{*\,2}} \in \mathbb{R})$

$\Rightarrow$ the effect of the moving sinks on the sources dominates the effect of the moving sources on the sinks

$\Rightarrow$ when c is small, we can just consider the correction to a stationary source

Eigenvalue Structure of Stationary Sources and Sinks

Stationary sources and sinks satisfy

$$\begin{aligned} d^2\hat{r}/dz^2 + \hat{r}\left(1 - \hat{r}^2 - \hat{\psi}^2\right) &= 0 \\ d\hat{\psi}/dz + K - \omega_1\hat{r}^2 + 2\hat{\psi}(d\hat{r}/dz)/\hat{r} &= 0. \end{aligned}$$

Linearise about the wavetrain

$\Rightarrow$ stationary sources decay to the wavetrain at rate $\sqrt{2}$
& stationary sinks decay to the wavetrain at rate $1/\sqrt{2} \pm i\delta/4$

$(\delta = \sqrt{11 - 12R^{*2}} \in \mathbb{R})$

$\Rightarrow$ the effect of the moving sinks on the sources dominates the effect of the moving sources on the sinks

$\Rightarrow$ when c is small, we can just consider the correction to a stationary source

Eigenvalue Structure of Stationary Sources and Sinks

Stationary sources and sinks satisfy

$$\begin{aligned} d^2\widehat{r}/dz^2 + \widehat{r}\left(1 - \widehat{r}^{\,2} - \widehat{\psi}^{\,2}\right) &= 0 \\ d\widehat{\psi}/dz + K - \omega_1 \widehat{r}^{\,2} + 2\widehat{\psi}\,(d\widehat{r}/dz)/\widehat{r} &= 0. \end{aligned}$$

Linearise about the wavetrain

$\Rightarrow$ stationary sources decay to the wavetrain at rate $\sqrt{2}$
& stationary sinks decay to the wavetrain at rate $1/\sqrt{2} \pm i\delta/4$

$(\delta = \sqrt{11 - 12R^{*\,2}} \in \mathbb{R})$

$\Rightarrow$ the effect of the moving sinks on the sources dominates the effect of the moving sources on the sinks

$\Rightarrow$ when c is small, we can just consider the correction to a stationary source

Eigenvalue Structure of Stationary Sources and Sinks

Stationary sources and sinks satisfy

$$\begin{aligned} d^2\widehat{r}/dz^2 + \widehat{r}\left(1 - \widehat{r}^{\,2} - \widehat{\psi}^{\,2}\right) &= 0 \\ d\widehat{\psi}/dz + K - \omega_1\widehat{r}^{\,2} + 2\widehat{\psi}\,(d\widehat{r}/dz)/\widehat{r} &= 0. \end{aligned}$$

Linearise about the wavetrain

$\Rightarrow$ stationary sources decay to the wavetrain at rate $\sqrt{2}$
& stationary sinks decay to the wavetrain at rate $1/\sqrt{2} \pm i\delta/4$

$(\delta = \sqrt{11 - 12R^{*\,2}} \in \mathbb{R})$

$\Rightarrow$ the effect of the moving sinks on the sources dominates the effect of the moving sources on the sinks

$\Rightarrow$ when c is small, we can just consider the correction to a stationary source: $r = R^*|\tanh(z/\sqrt{2})|$

Perturbation Theory Calculation

The wave speed is a natural small parameter........

Perturbation Theory Calculation

The wave speed is a natural small parameter........

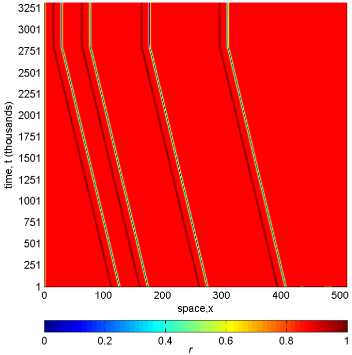

Perturbation Theory Calculation

The wave speed is a natural small parameter........

..........but
$\epsilon = [\frac{1}{2}(R_1 + R_2) - R^*] \cdot (\text{constant})$
is a better choice, where R^* is the amplitude of the stationary source.

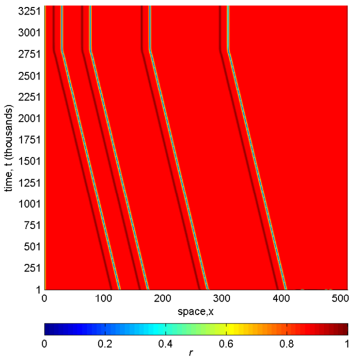

Perturbation Theory Calculation

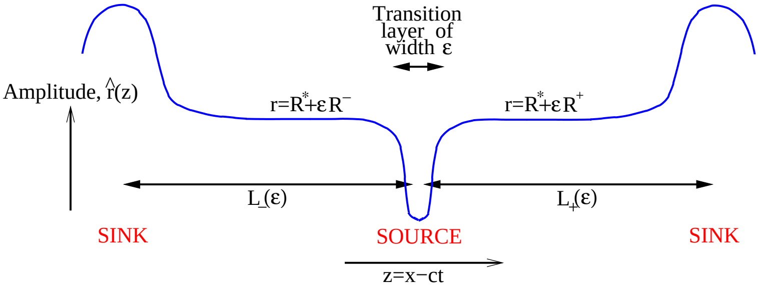

$$\text{For } \epsilon = 0: c = 0$$
$$K = (9-\sqrt{81+72\omega_1^2})/(4\omega_1)$$
$$\widehat{r} = R^*|\tanh(z/\sqrt{2})|$$
$$\widehat{\psi} = -(1-R^{*2})^{1/2}\tanh(z/\sqrt{2})$$

Perturbation Theory Calculation

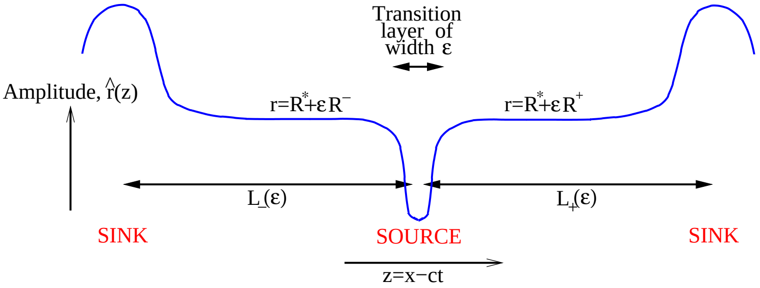

$$\begin{aligned}
\text{For } \epsilon \neq 0 : c &= \epsilon c_1 + O(\epsilon^2) \\
K &= (9-\sqrt{81+72\omega_1^2})/(4\omega_1) + \epsilon K_1 + O(\epsilon^2) \\
\hat{r} &= R^*|\tanh(z/\sqrt{2})| + \epsilon \hat{r}_1(z) + O(\epsilon^2) \\
\hat{\psi} &= -(1-R^{*\,2})^{1/2}\tanh(z/\sqrt{2}) + \epsilon\hat{\psi}_1(z) + O(\epsilon^2)
\end{aligned}$$

Perturbation Theory Calculation

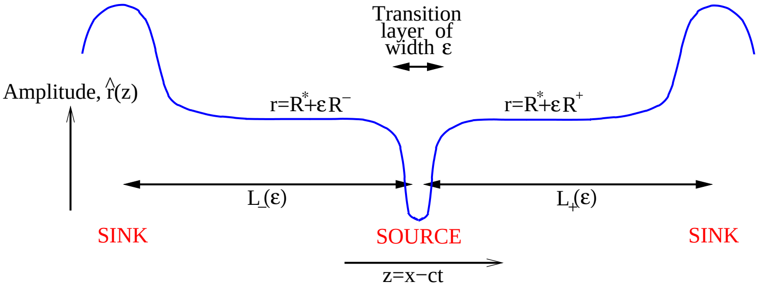

Results: $L_\pm(\epsilon) = -\sqrt{2}\log|\epsilon| - \sqrt{2}\log\kappa_\pm + o(1)$

where $\kappa_- \exp\{+i\delta\log\kappa_-\} + \kappa_+ \exp\{+i\delta\log\kappa_+\} = A$

A is a (complex) constant, independent of c_1, $O(1)$ as $\epsilon \to 0$

(recall that $\delta = \sqrt{11 - 12R^{*\,2}} \in \mathbb{R}$)

Outline

A Family of Moving Sources and Sinks

There is a three parameter family of moving sources and sinks:

Parameter 1: ϵ, which reflects the difference in wavetrain amplitudes

Parameter 2: c_1, which reflects the speed of movement

Parameter 3: $\kappa_\pm$, which refects the $O(1)$ contribution to the source-sink separation

Implications for the PDE Solutions

- Source-sink separations are variable. This corresponds to different values of $\kappa_{\pm}$ associated with different sources.

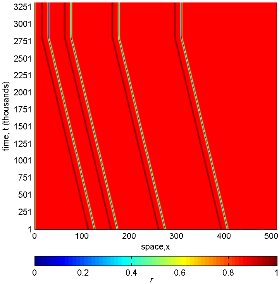

Implications for the PDE Solutions

- Source-sink separations are variable. This corresponds to different values of $\kappa_\pm$ associated with different sources.
- The sources and sinks all stop moving at (approximately) the same time. This is expected: all are part of a single travelling wave solution.

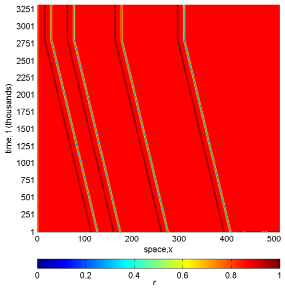

Implications for the PDE Solutions

- Source-sink separations are variable. This corresponds to different values of $\kappa_\pm$ associated with different sources.
- The sources and sinks all stop moving at (approximately) the same time. This is expected: all are part of a single travelling wave solution.

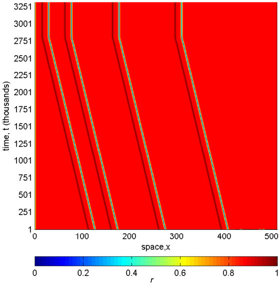

- There is (approximately) no change in the source-sink separation when the sources and sinks stop moving. This is because the equation for $\kappa_\pm$ does not involve the parameter c_1.

Implications for the PDE Solutions

- What is the distance between the leading sink and the $x = 0$ boundary when the sources and sinks stop moving? A minor adaptation of the calculation shows that the separation $L_{bdy}(\epsilon)$ is $-\sqrt{2}\log|\epsilon| - \sqrt{2}\log\kappa_{bdy} + o(1)$

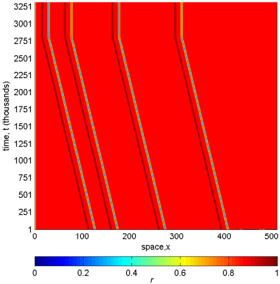

where $\mathrm{Im}\left[\overline{\sigma_2}\kappa_{bdy}\exp\left\{+i\delta(\log|\epsilon| + \log\kappa_{bdy})\right\}\right] = \mathrm{sign}(\epsilon)$

(σ_2 is a (complex) constant; recall $\delta=\sqrt{11-12R^{*\,2}}\in\mathbb{R}$)

Overall Conclusion

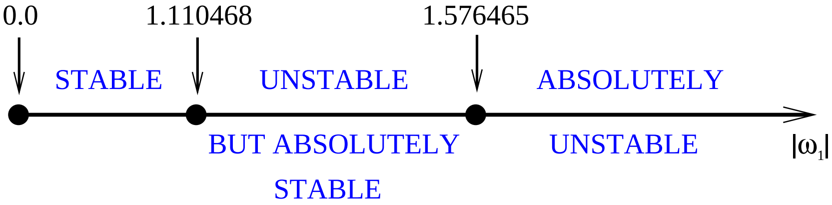

WAVETRAIN

PATTERNS OF SOURCES AND SINKS

DISORDERED SPATIOTEMPORAL OSCILLATIONS

Objectives for Future Work

- A better understanding of how a particular member of the family of moving sources and sinks is selected.
- A better understanding of the disordered solutions in the absolutely unstable parameter regime.

List of Frames